Nondestructive monitoring of fatigue damage evolution in austenitic stainless steel by positron-lifetime measurements

Uwe Holzwarth and Petra Schaaff
European Commission, Joint Research Centre, Institute for Health and Consumer Protection, Via E. Fermi 1 (T.P. 500), I-21020 Ispra (VA), Italy

(Received 21 April 2003; revised manuscript received 17 December 2003; published 12 March 2004)

Positron-lifetime measurements have been performed on austenitic stainless steel during (i) stress- and (ii) strain-controlled fatigue experiments for different applied stress and strain amplitudes, respectively. For this purpose a generator-detector assembly with a ^{72}Se/^{72}As positron generator [maximum activity 25 μCi (0.9 MBq)] has been mounted on mechanical testing machines in order to measure the positron lifetime without removing the specimens from the load train. The average positron lifetime has been determined by a $\beta^+ - \gamma$ coincidence. The feasibility to use the average positron lifetime for monitoring the evolution of fatigue damage and to predict early failure has been examined. In strain- and stress-controlled experiments the average positron lifetime shows a pronounced increase within the first 10% and 40% of the fatigue life, respectively. In stress-controlled experiments the average positron lifetime at failure depends significantly on the applied stress amplitude. In strain-controlled experiments significantly different positron lifetimes for different applied plastic strain amplitudes are obtained within the first 1.000 fatigue cycles, whereas differences get wiped out during further cycling until failure.

DOI: 10.1103/PhysRevB.69.094110 PACS number(s): 78.70.Bj, 61.72.Hh, 81.70.−q, 81.40.Np

I. INTRODUCTION

A. Nondestructive assessment of fatigue damage

Fatigue of materials is still a major engineering problem causing considerable economic damage and sometimes loss of human life.[1] A lot of research effort is going into the development of new nondestructive testing methods to characterize fatigue damage in materials, to predict residual service lifetime and to enhance safety standards for components subjected to alternating mechanical load.[1,2] In particular methods sufficiently sensitive for nondestructive detection of early stages of fatigue are still missing.[2] Most of the common techniques become sensitive to fatigue damage shortly before failure when microscopic cracks are already present and crack coalescence and accelerated crack growth start. Sensitive methods like x-ray line broadening require polished surfaces, and Barkhausen noise is confined to ferromagnetic materials. X-ray diffraction, eddy currents, or ultrasound methods measure the effect of dislocations, atomic defects, defect clusters, or microcracks on physical properties like interlattice plane distance, electrical resistivity, or sound propagation. On the other hand, positron annihilation is highly sensitive to vacancylike defects such as lattice vacancies or dislocations, and can detect them at such low densities that they hardly start to measurably change the physical material properties measured by the above mentioned techniques. In this sense, positron annihilation is a more direct and more sensitive method to measure deformation damage.

B. Positron annihilation in plastically deformed metals

The high sensitivity of positrons to plastic deformation is well known in metals[3,4] since the 1960s. A summary of the first two decades of research has been given by Byrne.[5]

The interaction of positrons with different types of crystal defects has been subject of intense research (see Refs. 6–9). Positron capture in single vacancies is the best understood process because vacancies can be created and investigated in thermal equilibrium at elevated temperatures without interferences by presence of other types of defects. Plastic deformation does not exhibit such an advantage because the production of dislocations and vacancies is always interconnected.[10–12] Therefore, the interpretation of positron annihilation data measured in plastically deformed metals is not straightforward. Starting with a well annealed metal, the dislocation density increases by several orders of magnitude during a tensile test or a fatigue experiment. In both cases the positron lifetime and the Doppler broadening of the 511-keV annihilation radiation show significant changes.[5] One is tempted to attribute the measured effect to annihilation of positrons trapped in the dilatational zone of dislocations. More recent experimental (e.g., Refs. 13–18) and theoretical (e.g., Refs. 19–21) investigations, however, agree that dislocations in many metallic materials are too shallow traps to effectively bind positrons at room temperature.

For edge dislocation lines in copper, nickel, aluminum, and zinc typical binding energies of 5 meV$\leqslant E_b \leqslant$100 meV have been determined.[13,14,16,19] In positron lifetime measurements performed at 77 K after tensile deformation of α-iron single crystals at 200 K Park *et al.*[22] could determine separately the densities of screw and edge dislocations after identifying positron lifetimes of 165 and 143 ps for positrons trapped in edge and screw dislocations, respectively. This agrees with earlier findings that the lifetime of positrons trapped in the dilatational zone of an edge dislocation at low temperature is just slightly smaller than that of a single vacancy in the same material.[23–25] Measurements at low temperatures are however not convenient for nondestructive testing purposes.

In the presence of dislocations an enhanced trapping rate of positrons into vacancies has been found.[23,26,27] Therefore, Doyama and Cotterill[25] suggested considering dislocation

lines at room temperature rather as precursor states for a transition into deeper traps such as vacancies trapped in the elastic stress field around a dislocation or (monoatomic) jogs on edge dislocation lines, for which a positron lifetime slightly lower to those in vacancies have been calculated,[19] than the final annihilation site.[15,28,29] The consequences of this model, especially on the temperature dependence of the positron trapping rate at dislocations, were discussed by several authors.[16,30,31] From this we conclude that the high sensitivity of positron annihilation measurements performed at room temperature to plastic deformation originates from the vacancies produced by dislocation processes such as dragging of jogs on screw dislocations[10,11] or by the annihilation of edge dislocations.[33]

C. Evolution of fatigue microstructures

In fatigue of metals the evolution of the densities of vacancies, vacancy agglomerates, and jogs as possible positron trapping sites is superimposed on the evolution of dislocation cells or peculiar dislocation patterns like persistent slip bands.[32] This leads to a modulation of the dislocation density by a factor of 10^2–10^4 on a length scale of a few μm. The evolution of the spatial distribution of dislocations has been extensively studied by transmission electron microscopy (TEM) and has been reviewed by various authors.[34–40] Fatigue microstructures are characterized by regions with high dislocation densities [between about 5×10^{15} m^{-2} (Ref. 41) and 1.4×10^{17} m^{-2} (Ref. 42)] that are separated by dislocation poor regions (typically 5×10^{12} m^{-2}). However, the densities of vacancies or monoatomic jogs on dislocation lines as candidates for positron trapping are not accessible by TEM and the evolution of their densities is difficult to predict: Where edge dislocations annihilate, the locally high density of atomic defects (vacancies and interstitials) is supposed to favor the formation of defect clusters (e.g., Refs. 33 and 43–45). When sufficiently mobile, vacancies may move to sinks such as surfaces, grain or phase boundaries, dislocations or other atomic defect clusters. Moving dislocations may pick up immobile vacancies or cut through atomic defect clusters thereby segmenting them.[33] The absorption of vacancies or interstitials on an edge dislocation line creates monoatomic jogs. The absorption of atomic defects at such jogs moves the jog by one atomic distance along the dislocation line.

In spite of reports on the TEM observation of spherical vacancy clusters in fatigued metals (e.g., Refs. 43 and 45), in many observations vacancy clusters show the contrast behavior of Frank dislocation loops.[42] Unfortunately, with the exception of neutron diffraction[46] or x-ray diffraction[47] there are no other independent experimental techniques than positron annihilation that are sufficiently sensitive and specific to detect atomic defect clusters.

A quantitative modelling of the production of single vacancies is so far restricted to simple conditions of homogeneously distributed dislocations[48] experimentally realized by weak, uniaxial tensile deformation before dislocation bundles become too dense or cell structures start to form.[49–51] According to the authors' knowledge modeling approaches that could deliver quantitative data on the evolution of the densities of jogs and vacancies during fatigue experiments are not yet available in spite of progress in modeling and computer simulations of dislocation patterning in fatigue.[52] On the other hand, positron annihilation could appreciably contribute to an experimental verification of such models.

An important feature of fatigue is a state of cyclic saturation reached in most materials provided cyclic load is sufficiently low not to immediately cause growth of preexisting (surface) flaws. In strain-controlled experiments cyclic saturation is characterized by a plateau in the cyclic hardening curve, i.e., the presentation of the stress amplitude versus the number of fatigue cycles.[32] Analogously, in stress-controlled experiments the strain amplitude is expected to become constant when cyclic saturation is reached. In annealed materials the dislocation density will initially strongly increase, and the material hardens, whereas, e.g., in cold worked materials it can also undergo an initial reduction usually reflected in a negative cyclic hardening, i.e., cyclic softening. When cyclic hardening or softening curves reach a plateau a dynamic equilibrium between dislocation production and annihilation is reached (see, e.g., Ref. 40). Measurements of the electrical resistivity at 4.2 K during fatigue of copper single crystals provide evidence that also the concentration of atomic defects reaches a dynamic equilibrium.[42,53] Consequently, the evolution of the density of positron trapping sites is expected to reach a dynamic equilibrium too.

D. Positron annihilation in fatigued metals

The literature on the fatigue of copper and other, mainly pure, metals with a face-centered-cubic crystal structure is rich and also various positron annihilation studies were already performed (e.g., Refs. 5, 44, and 54). In well annealed copper single crystals fatigued at small total strain amplitudes below 1×10^{-4} the sensitivity threshold for positron annihilation of about 10^{-7} vacancies per atom[8] is exceeded within a few thousand fatigue cycles,[17] which is less than 1% of the fatigue life. The dynamics of production and annihilation of vacancies in fatigue experiments is determined by the dynamics of dislocation motion and multiplication, and therefore depends strongly on the initial microstructure. Hence, it appears clear that changes of microstructure due to fatigue hardening and softening can be revealed with positron annihilation as has been demonstrated for copper,[17,44,54] nickel,[55,56] and technically more relevant materials like stainless steels[57–59] and AISI 4340 steel.[60]

E. Choice of material

The present investigation deals with the low-carbon austenitic stainless steel type AISI 316 L (American Iron and Steel Institute specification). The fatigue behavior of this material has extensively been studied for nuclear energy applications including TEM studies.[61–66] It remains a single phase austenitic material under all application conditions relevant to this study. Therefore, the evaluation of positron-lifetime measurements does not need to consider deformation induced phase transformations. S-parameter measurements by

TABLE I. Chemical composition of stainless steel AISI 316 L according to the supplier certificate.

Elements	C	Si	Mn	Ni	Cr	Mo	S	P	Fe
wt %	0.018	0.582	1.676	11.13	17.38	2.151	0.002	0.021	67.04
at %	0.08	1.15	1.69	10.53	18.57	1.24	0.01	0.04	66.68

Gauster *et al.*[57] after isochronous annealing of stainless steel specimens cold rolled to 25% thickness reduction, accompanied by TEM and Knoop microhardness measurements, showed that annealing starts around 430 K, but no dislocation annealing occurred below 873 K. Positron lifetime measurements on specimens, fabricated from the same stainless steel batch used for the experiments presented here, deformed in compression and annealed in isochronous steps, revealed vacancies as the only relevant positron traps at room temperature.[67] There is no evidence of direct trapping of positrons to dislocation lines at room temperature in AISI 316 L stainless steel.

F. Positron annihilation in nondestructive testing

Several attempts have been reported in literature to develop systems for nondestructive testing using positron-lifetime measurements by a $\beta^+ - \gamma$-coincidence technique[68,69] or positron annihilation line shape analysis.[69–75] The experimental set-up of a ^{72}Se/^{72}As positron generator for nondestructive measurements used in the present paper has already been presented,[68] as well as preliminary results on *in situ* positron-lifetime measurements during fatigue of stainless steel AISI 316 L.[59]

The present paper presents a comparison of positron annihilation data of stress- and strain-controlled fatigue experiments with a special emphasis on experimental reproducibility. So far, most positron annihilation studies on fatigue present only single sets of experiments. And in some publications different stages of fatigue life under nominally identical fatigue parameters are established and probed in different specimens (e.g., Refs. 58 and 69). The large amount of measurements in the present paper has been economically affordable only due to the truly nondestructive technique that avoids time consuming specimen preparation. It will be shown that positron annihilation could be helpful also concerning various aspects of research in basic fatigue mechanisms.

It should be emphasized that the complex of fracture mechanics is not touched upon in the present publication since we consider crack growth and crack propagation as phenomena of late fatigue life that can be examined by the already applied nondestructive testing tools.

II. EXPERIMENTAL PROCEDURES

A. Material and specimen preparation

The stainless steel AISI 316 L was supplied by Creusot–Loire in plates of 1×2 and 30-mm^3 thickness. The material composition as specified by Creusot–Loire, is given in Table I. The plates had been hot rolled, solution annealed at 1050 °C for 30 min in order to dissolve carbides and then quenched by submersion of the plates in cold water in order to avoid their recreation by migration of carbon atoms in the austenitic matrix. According to the chromium and nickel equivalents calculated after Pryce and Andrews,[76] the content of ferrite was about 1% only. Metallography showed that the ferrite was localized in stringers parallel to the rolling direction of the material. The average grain size of the material has been determined according to ASTM E112 (Ref. 77) by the linear intercept method and was found to be 40–50 μm. From these plates bars of $30\times30\times170$ mm^3 were cut by spark erosion and cylindrical fatigue specimens with tangentially blending fillets between the gauge length and the gripping parts were machined. The specimen axis was parallel to the rolling direction.

Specimen shapes and the execution of the fatigue tests complied with the ASTM Standard E 466 (''Conducting Constant Amplitude Axial Fatigue Tests of Metallic Materials'') and ASTM Standard E 606 (''Standard Recommended Practice for Low-Cycle Fatigue Testing'').[77] The fabrication process of the specimens by machining is compatible with the cited ASTM Standards. The resulting surface finish on the gauge length exhibited a maximum roughness of 0.2–0.25 μm. Two types of specimen geometries were used since the fatigue testing systems were equipped with different specimen grips. Specimens for the experiments on the Instron servohydraulic testing system type 1273 and on the MTS system 810 with maximum load capacity of 250 kN were of type A in Fig. 1. The specimens used on the MTS system 810 with maximum load capacity of 50 kN were button headed specimens of type B (cf. Fig. 1).

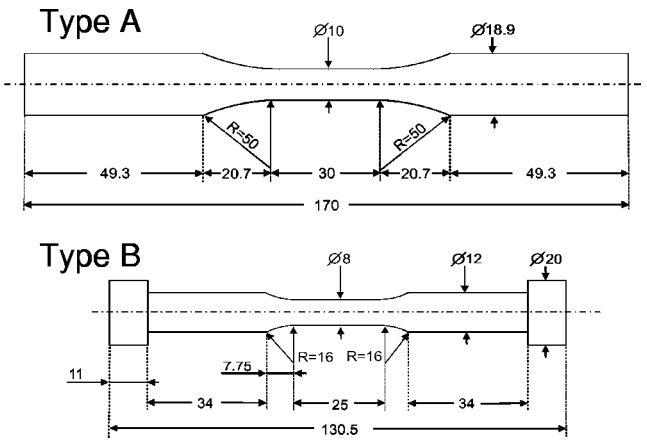

FIG. 1. Specimen shape (type A) used for the fatigue experiments on the servohydraulic testing systems Instron type 1273 and MTS type 810 (250 kN). Specimen shape (Type B) used for stress- and strain-controlled fatigue experiments on the servohydraulic testing systems MTS type 810 (50 kN).

In spite of solution annealing and quenching from 78% of the melting temperature (1425 °C) of stainless steel AISI 316 L,[78] the residual concentration of vacancies was low. An estimate of the thermodynamic equilibrium concentration at the solution annealing temperature, based on a typical vacancy concentration of 5×10^{-4} in thermodynamic equilibrium at the melting point,[79] and a vacancy formation enthalpy $H_V^F=1.61$ eV (Ref. 80) yields an equilibrium concentration of about 2×10^{-5} at the annealing temperature (1050 °C). However, the achievable cooling rate by water quenching in the center of a 30-mm-thick large plate, where the specimens stem from, is too low to preserve this concentration due to the low thermal conductivity of stainless steel [13.95 $W\,m^{-1}\,K^{-1}$ (Ref. 78)]. Only a few percent of the equilibrium concentration is preserved. The concentration of vacancies in a Fe-Cr-Ni alloy after quenching from 1050 °C has been estimated by Wang *et al.*[81] to be about 10^{-6}.

B. Cyclic deformation—fatigue

The primary control parameters in stress- and strain-controlled experiments are the axial stress σ and the total axial elongation ε_{tot}, respectively. σ is calculated from the axial force F, measured by a load cell, divided by the cross sectional area A of the specimen on the gauge length. Symmetric push-pull fatigue experiments ($\sigma_{min}/\sigma_{max}=-1$) were performed under load control at nominal stress amplitudes in the range between 220 and 290 MPa with a sinusoidal command wave. The cycling frequency was 10 Hz. For the present material and testing conditions the fatigue limit, defined as the stress amplitude where 50% of the specimens reach 1×10^7 cycles without failure was found to be 225 MPa.[82]

ε_{tot} is calculated from the elongation Δl along a segment of the length $l_0=10$ mm in the center of the gauge length according to $\varepsilon_{tot}=\Delta l/l_0$. l_0 was determined by the dimension of the MTS clip-on extensometer used to measure Δl. The total strain ε_{tot} consists of elastic (ε_{el}) and plastic (ε_{pl}) contributions. The elastic part follows Hooke's law of linear elasticity and can be calculated from the stress σ and the Young's modulus E that can be derived from the slope of the linear part of the stress-strain curve of the material. The plastic strain ε_{pl} can be related to microscopic dislocation quantities like the density of mobile dislocations $N_{d,m}$ and their average velocity $v_{d,m}$ by the Orowan relation[83]

$$\dot{\varepsilon}_{pl}=b\cdot N_{d,m}\cdot v_{d,m}. \tag{1}$$

Here, b denotes the modulus of the Burgers vector of the mobile dislocations. For polycrystalline materials averaging procedures are required to extract quantitative information from Eq. (1).

Experiments under control of plastic strain rate are preferred in materials science when aiming at the best possible control of microstructure evolution. For this purpose, the plastic strain has been calculated on line from the simultaneous measurement of the total strain ε_{tot} and the stress σ according to

$$\varepsilon_{pl}=\varepsilon_{tot}-\varepsilon_{el}=\varepsilon_{tot}-\frac{\sigma}{E}, \tag{2}$$

and a constant plastic strain rate $\dot{\varepsilon}_{pl}$ has been assured by using a triangular command wave for ε_{pl}. Strain-controlled fatigue experiments ($\varepsilon_{pl,min}/\varepsilon_{pl,max}=-1$) were performed for plastic deformation amplitudes in the range between 1×10^{-4} and 5×10^{-3} with a triangular command wave using servohydraulic MTS systems. The cycling frequency was limited to 0.5 Hz in order to exclude gliding of the clip-on extensometer on the specimen surface. For simplicity, from now on, σ and ε_{pl} shall denote the applied stress amplitude and the applied plastic strain amplitude, respectively.

C. Expanded work of cyclic deformation

Since positrons are sensitive to vacancylike defects the average positron lifetime will saturate (i) if all positrons are trapped in defects (saturation trapping) or (ii) if the density of relevant positron traps saturates. Since the latter is expected to occur in cyclic saturation the hysteresis loops were examined. Moreover, the area under the hysteresis loop

$$\oint \sigma\,d\varepsilon_{pl}=\oint \sigma\,d\varepsilon_{tot}=w \tag{3}$$

gives the work of deformation w required per deformation cycle. w has the dimension of an energy density and multiplication with the volume $V=A\cdot l_0$ gives the work of deformation W that is supplied by the servohydraulic fatigue machine into the part of the gauge length controlled by the clip-on extensometer. The integration over ε_{pl} and ε_{tot} gives the same result because the presentation of a hysteresis loop in a plot of σ versus ε_{tot} can be transformed into a presentation of σ versus ε_{pl} by equiareal mapping, i.e., by a shearing operation with respect to the elastic straight line with slope E.

In cyclic saturation this energy is dissipated by the material and completely transformed into heat. Before cyclic saturation is reached a certain fraction of this energy is stored in the material by producing defects like dislocations, vacancies, and interstitials. In terms of the dissipated heat q and the stored energy e per unit volume the simple relation $w=q+e$ holds. It has been demonstrated by Mughrabi[84] that the shape of the hysteresis loop and consequently its area may vary even for constant values for the registered amplitudes ε_{pl} and σ. Therefore, the variation of the area of the hysteresis loops as function of the number of fatigue cycles N is more significant for our purposes than the simple coregistration of the stress or strain amplitude in strain- or stress-controlled experiments, respectively.

D. Positron lifetime measurements

The fatigue machines have been equipped with a mobile positron beam to perform positron-lifetime measurements without removing the specimen from the load train. The system was mounted and adjusted in a way to measure always on the same site in the center of the gauge length. Fatigue cycling was stopped for positron-lifetime measurements after

100*, 200*, 500, 1000, 2000, 5000, and 10000 cycles, and so on in a logarithmic sequence (* indicates measurements that were skipped in later experiments, when early changes of τ_{av} were expected to be negligible). The last measurements were performed after failure of the specimens.

The experimental setup of the mobile positron beam and the production of the miniaturized positron sources used for the present experiments were already described in detail elsewhere.[17,68] A ^{72}Se/^{72}As generator with a maximum initial activity of about 25 μCi ($\approx$0.9 MBq) was used as positron source. The ^{72}Se was vapor deposited inside a small gold cylinder of 0.6-mm inner diameter acting as the beam collimator. This gold cylinder was integrated in the tip of a plexiglass light guide on top of a photomultiplier tube and covered with a plastic scintillator which produces a scintillation start signal only for those positrons that are emitted in the direction towards the specimen under examination. The setup was shielded against light by a 12-μm-thick aluminum foil. A specimen in a distance of 3 mm from the tip of the collimator was subjected to positron irradiation in an area of 3.6 mm in diameter. The stop signal was delivered by a BaF_2 crystal after registration of the 511-keV annihilation quanta. Signal processing was done by a fast-slow coincidence measurement as described earlier.[17,68] The electronic equipment was housed in a cabinet kept at constant temperature of 20 $\pm$0.5 °C.

^{72}As emits two positron spectra with maximum energies of 2.5 and 3.3 MeV.[85] Estimating the most probable positron energy from 1/3 of the maximum energy of the spectra, and subtracting an energy loss of 150 keV for the passage of the plastic scintillator, gives penetration depths of 370 and 550 μm into stainless steel for the 2.5- and 3.3-MeV spectra, respectively. The positron annihilation data obtained in this way are more representative of the bulk properties of a material than those obtained by the classical methods with ^{22}Na with a maximum positron energy of 544 keV. Compared with the sandwich technique using a ^{22}Na source and a γ-γ coincidence the present technique exploits a much smaller solid angle. The effect on count rate is, however, largely compensated for by the higher efficiency of the β-γ coincidence and the higher (initial) source strength of the ^{72}Se/^{72}As generator.

The ^{72}Se/^{72}As generator offers the possibility to register simultaneously a prompt γ quantum of the 835 keV emitted by ^{72}Ge and to monitor the stability of the detection system and its time resolution. The time resolution of the instrument has been determined as the full width half maximum of the 835 keV prompt line. Alternatively, a Gaussian curve has been fitted to the prompt line. Both methods yield a time resolution of 230$\pm$5 ps.

For the positron-lifetime measurements the cyclic deformation has been paused and the specimens have been shielded with plexiglass that captured all positrons missing the specimen or being reflected from its surface. The average positron lifetime in plexiglass of about 1500 ps is sufficiently different from the average positron lifetimes expected in a metal of 100–200 ps that an easy background correction can be performed by weighted subtraction of a plexiglass reference spectrum. Reference spectra have been recorded periodically by replacing the steel specimen in the load train by a plexiglass dummy. In this way constant geometry has been assured and the effect of the background correction on the accuracy of the determination of τ_{av}, that is susceptible to possible electronic drift effects, has been checked periodically. The weighting factor has been determined from the ratio of counts in a window of the spectrum, in which the spectrum was determined by very long-lived contributions only, and the counts in the same window in the reference spectrum. For this background correction the width of the windows and their position with respect to the center of the annihilation spectra were identical. This method also corrects the annihilation events of low energy positrons in the scintillation start detector and the aluminum foil shielding the photomultiplier tube from daylight.

Before correction each spectrum contained 1.1×10^6 coincidence events. The required acquisition time increased from initially about 20 min to more than 2.5 h after four weeks due to the 8.4 days half-life of the ^{72}Se/^{72}As generator. Typically 55–60 % of these events were lost by the weighted subtraction of the reference spectrum. The average positron lifetime has then been evaluated by a weighted linear regression to the linear part of the spectrum (in logarithmic presentation). The statistical error of the fits was less than 1 ps. However, the overall accuracy is $\pm$3 ps due to the reproducibility of the experiments when positron lifetime spectra of the same specimen (state) have been recorded repeatedly during the measurement campaign and due to slight differences in the positron lifetime values when minimizing the statistical error by varying the position of the windows for background correction and the weighted linear regression. When all measurements were completed after a fatigue test a final evaluation of τ_{av} of all spectra was conducted with identical windows for background correction and linear regression fit.

A systematic decomposition of the average positron lifetime into different components has not been performed, since at least twice the number of coincidence events are recommended for a stable decomposition in more lifetime components.[86] Moreover, additional experimental techniques like neutron diffraction would be required to gain further information on type and configuration of positron trapping sites.

III. RESULTS

A. Stress- and strain-controlled experiments

All performed stress- and strain-controlled experiments are presented in Fig. 2 as Wöhler plots of the applied stress amplitude σ and the applied plastic strain amplitude ε_{pl} versus the number of load cycles till failure N_f, respectively. Experiments stopped before failure are included and marked with open symbols. All relevant experimental details are compiled in Tables II and III for stress- and strain-controlled experiments, respectively. Lines presented in the figures are eye guides only to improve apprehension of the data.

In Figs. 3 and 4 the evolution of the average positron lifetime during stress- and strain-controlled fatigue experiments on stainless steel AISI 316 L is presented, respectively.

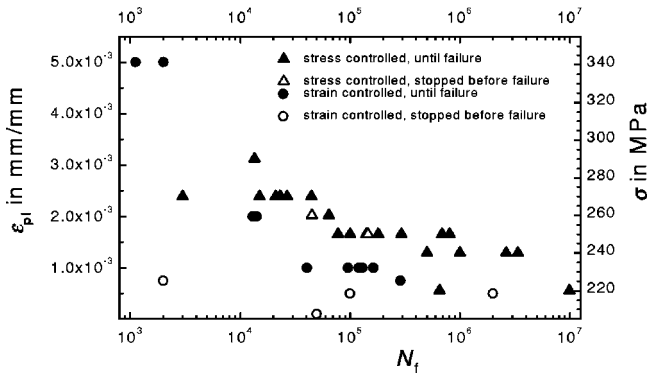

FIG. 2. Presentation of all executed stress- and strain-controlled experiments that underwent positron annihilation measurements, as stress and strain amplitude, right- and left-hand sides, respectively, vs fatigue life given by the number of load cycles until failure N_f (filled symbols). Open symbols denote experiments that were stopped before failure.

The error bars in Figs. 3 and 4 denote the accuracy of the measurement. In order to keep the figures clear, error bars are presented for every second experiment only. In order to keep a logarithmic scale for the number of fatigue cycles N the average positron lifetime $\tau_{av}(0)$ in the undeformed initial state at $N=0$ is reported at $N=10^0$. Plastic deformation of a surface layer during machining caused a scatter of the average positron lifetime in the initial state,[67] $\tau_{av}(0)$, as indicated in Tables II and III. Since we renounced electrolytic or chemical polishing after machining, the scatter of the initial average positron lifetime $\tau_{av}(0)$ was larger than the accuracy of the average positron lifetime measurement of ± 3 ps. In order to check the influence of the scatter of $\tau_{av}(0)$ on the information to be derived from our experiments in Figs. 5 and 6, the experiments shown in Figs. 3 and 4 are presented as an increase of the average positron lifetime, $\Delta\tau_{av}(N) = \tau_{av}(N) - \tau_{av}(0)$, with respect to their start value $\tau_{av}(0)$. These figures show convincingly that the scatter of $\tau_{av}(0)$

TABLE II. Summary of stress-controlled experiments. Presented are the stress amplitude σ, the fatigue life N_f, the initial average positron lifetime $\tau_{av}(0)$, the average positron lifetime at failure $\tau_{av}(N_f)$ and the increase until failure $\Delta\tau_{av}(N_f)$. Analogously, for experiments stopped after N_s cycles the average positron lifetime $\tau_{av}(N_s)$ and its increase $\Delta\tau_{av}(N_s)$ until N_s are given. The type of deformation system used, defined the specimen geometry (see Fig. 1). Since no electrolytical polishing or gentle grinding has been applied after the final machining of the specimens, $\tau_{av}(0)$ exhibits a scatter of (129 ± 5) ps, (110 ± 3) ps and (120 ± 5) ps for the specimen batches used on the systems Instron 1273, MTS 810 (250 kN) and MTS 810 (50 kN), respectively.

Label	σ in MPa	N_f	N_s	$\tau_{av}(0)$ in ps	$\tau_{av}(N_f)$ in ps	$\tau_{av}(N_s)$ in ps	$\Delta\tau_{av}(N_f)$ in ps	$\Delta\tau_{av}(N_s)$ in ps	Deformation system
A220	220		650000	129		127		2	Instron 1273
A230	220		10000000	130		151		19	Instron 1273
A240	240		2090000	131		160		29	Instron 1273
B240	240	3353570		129	155		26		Instron 1273
C240	240		500000	120		143		23	Instron 1273
D240	240		1000000	119		131		12	Instron 1273
A250	250	300000		133	172		39		Instron 1273
B250	250	687000		131	163		32		Instron 1273
C250	250	140226		112	141		29		MTS 810 (250kN)
D250	250	145621		110	146		26		MTS 810 (250kN)
E250	250		100000	125		147		22	MTS 810 (50kN)
F250	250	802300		125	146		21		MTS 810 (50kN)
G250	250	77635		120	152		32		MTS 810 (50kN)
H250	250	179916		n.a.					MTS 810 (50kN)
I250	250	291930		n.a.					MTS 810 (50kN)
A260	260	80000		127	170		43		Instron 1273
B260	260	44967		111	145		34		MTS 810 (250kN)
A270	270	23000		125	169		44		Instron 1273
B270	270	25000		131	160		29		Instron 1273
C270	270	23000		126	168		42		Instron 1273
D270	270	23000		138	186		48		Instron 1273
E270	270		3000	121		142		21	Instron 1273
F270	270		15000	123		160		37	Instron 1273
G270	270	45349		120	150		30		MTS 810 (50kN)
H270	270	21037		129	160		31		MTS 810 (50kN)
A290	290	13000		123	176		53		Instron 1273

TABLE III. Summary of all strain-controlled experiments. Presented are the plastic strain amplitude ε_{pl} in mm/mm, the fatigue life N_f, the initial average positron lifetime $\tau_{av}(0)$, the average positron lifetime at failure $\tau_{av}(N_f)$ and its increase until failure $\Delta\tau_{av}(N_f)$. Analogously, for experiments stopped after N_s cycles the average positron lifetime $\tau_{av}(N_s)$ and its increase $\Delta\tau_{av}(N_s)$ until N_s are given. Since no electrolytical polishing has been applied after the final machining of the specimens, $\tau_{av}(0)$ exhibits a scatter (110 ± 3) ps and (120 ± 5) ps for the specimen batches used on the systems MTS 810 (250 kN) and MTS 810 (50 kN), respectively.

Label	ε_{pl} in MPa	N_f	N_s	$\tau_{av}(0)$ in ps	$\tau_{av}(N_f)$ in ps	$\tau_{av}(N_s)$ in ps	$\Delta\tau_{av}(N_f)$ in ps	$\Delta\tau_{av}(N_s)$ in ps	Deformation system
A1E4	1×10^{-4}		50000	118		118		0	MTS 810 (50kN)
A5E4	5×10^{-4}		1000000	113		146		33	MTS 810 (50kN)
B5E4	5×10^{-4}		100000	125		136		11	MTS 810 (50kN)
C5E4	5×10^{-4}		2000000	113		143		30	MTS 810 (250kN)
A75E4	7.5×10^{-4}	278163		107	139		32		MTS 810 (250kN)
B75E4	7.5×10^{-4}		2000	113		145		32	MTS 810 (250kN)
A1E3	1×10^{-3}	40724		113	145		32		MTS 810 (50kN)
B1E3	1×10^{-3}	120500		119	139		20		MTS 810 (50kN)
C1E3	1×10^{-3}	163775		125	148		23		MTS 810 (50kN)
D1E3	1×10^{-3}	130220		115	158		43		MTS 810 (50kN)
E1E3	1×10^{-3}	95945		111	146		35		MTS 810 (50kN)
A2E3	2×10^{-3}	14141		114	148		34		MTS 810 (50kN)
B2E3	2×10^{-3}	13007		126	152		26		MTS 810 (50kN)
A5E3	5×10^{-3}	1120		132	162		30		MTS 810 (50kN)
B5E3	5×10^{-3}	2010		121	158		37		MTS 810 (50kN)

has no significant impact on the evolution of $\tau_{av}(N)$ and $\Delta\tau_{av}(N)$ during fatigue experiments. The error bars for $\Delta\tau_{av}(N)$ denote twice the accuracy of a positron lifetime measurement, i.e., ±6 ps because the result is the difference of two measurements.

In stress- and strain-controlled experiments the smallest deformation amplitude can be distinguished that has no significant effect on the average positron lifetime. This amplitude of 220 MPa, identified in the stress-controlled experiments, agrees well with the fatigue limit of 225 MPa derived from a Wöhler plot of specimens produced from the same batch of material and cyclically deformed under identical experimental conditions.[82] In strain-controlled experiments the lowest applied $\varepsilon_{pl}=1\times10^{-4}$ did not yield any significant change of τ_{av} up to 50.000 cycles. Therefore the experiment has been stopped and $\varepsilon_{pl}=1\times10^{-4}$ was considered as fatigue limit in strain control.

In stress- and strain-controlled experiments executed at values above the fatigue limit the average positron lifetime exhibits a pronounced increase during fatigue life. The higher the applied amplitude σ or ε_{pl} the higher is the increase rate $\Delta\tau_{av}/\Delta N$ especially during early fatigue life. In Figs. 7 and 8 the increase of the average positron lifetime

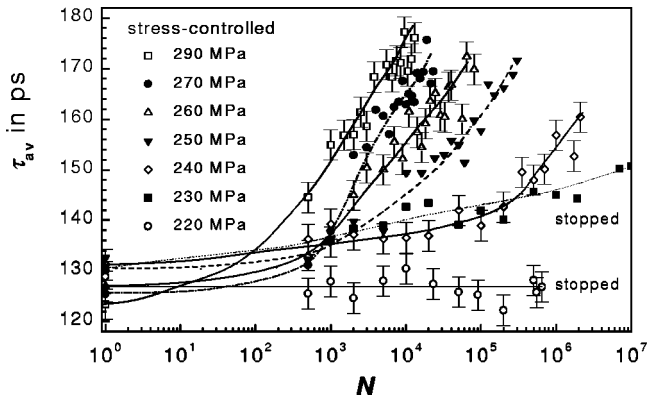

FIG. 3. Evolution of average positron lifetime τ_{av} during stress-controlled fatigue experiments for different applied stress amplitudes σ given in MPa [A series: A290, A270, A260, A250, A240, A230, and A220 (cf. Table II)]. The error bars denotes the accuracy of the positron lifetime measurement of ±3 ps. In order to keep the graph readable, they are presented for every second experiment only. *N* denotes the number of load cycles.

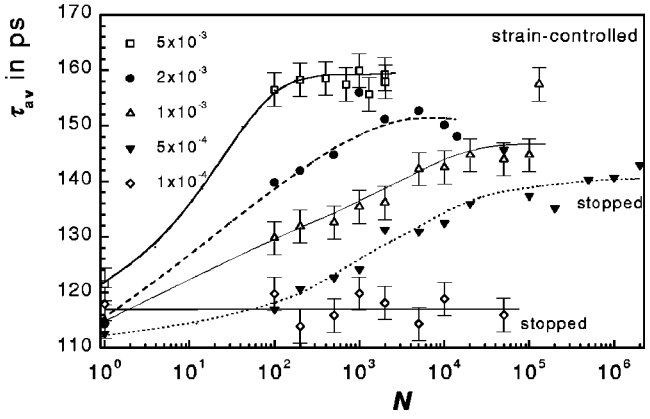

FIG. 4. Evolution of average positron lifetime τ_{av} during strain-controlled fatigue experiments for different applied plastic strain amplitudes ε_{pl} given in mm/mm [experiments B5E3, A2E3, D1E3, C5E4, and A1E4 (cf. Table III)]. The error bars denote the accuracy of the positron lifetime measurement of ±3 ps. In order to keep the graph readable, they are presented for every second experiment only. *N* denotes the number of load cycles.

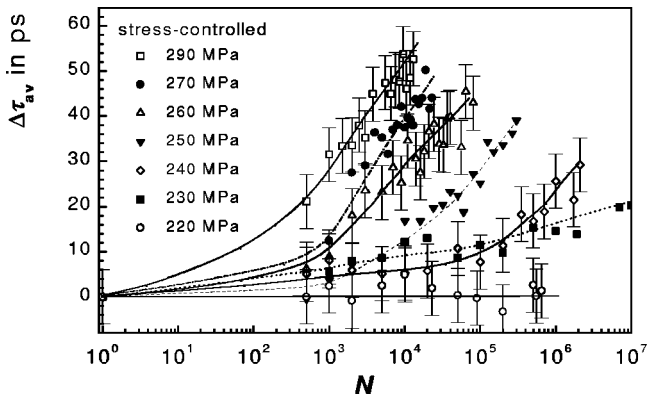

FIG. 5. Increase of the average positron lifetime $\Delta\tau_{av}(N) = \tau_{av}(N) - \tau_{av}(0)$ with respect to the initial value $\tau_{av}(0)$ at $N=0$ during the stress-controlled fatigue experiments presented in Fig. 3. The error bars given for every second experiment of ± 6 ps correspond to twice the accuracy of the positron lifetime measurement of ± 3 ps due to the calculation of the difference $\tau_{av}(N) - \tau_{av}(0)$. N denotes the number of load cycles.

normalized to the value at failure $\Delta\tau_{av}(N)/\Delta\tau_{av}(N_f)$ is plotted against the stage in fatigue life given by N/N_f. Only those experiments of Figs. 5 and 6 are presented that were continued until failure. In Fig. 7 a saturationlike behavior can be recognized in stress-controlled experiments after about 40% of fatigue life. All data registered later in fatigue life lie in a channel of less than $0.2 \cdot \Delta\tau_{av}(N_f)$ width. In this range the determined values of $\Delta\tau_{av}(N)$ are no longer significantly different. Strain-controlled experiments show a much earlier saturation as can be seen from Fig. 8. The main increase of the average positron lifetime occurs within the first 10% of fatigue life.

For the highest applied stress amplitude of 290 MPa a positron lifetime of $\tau_{av}(N_f) = 178$ ps was determined at failure. This is significantly higher than the 160 ps in the strain-controlled experiment with $\varepsilon_{pl} = 5 \times 10^{-3}$ although stress

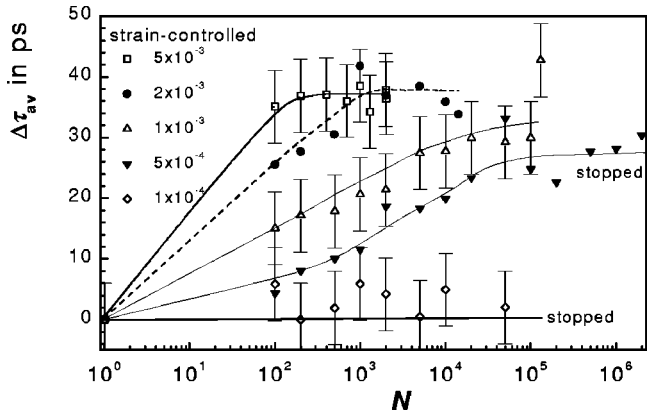

FIG. 6. Increase of the average positron lifetime $\Delta\tau_{av}(N) = \tau_{av}(N) - \tau_{av}(0)$ with respect to the initial value $\tau_{av}(0)$ at $N=0$ during the strain-controlled fatigue experiments presented in Fig. 4. The error bars given for every second experiment of ± 6 ps correspond to twice the accuracy of the positron lifetime measurement of ± 3 ps due to the calculation of the difference $\tau_{av}(N) - \tau_{av}(0)$. N denotes the number of load cycles.

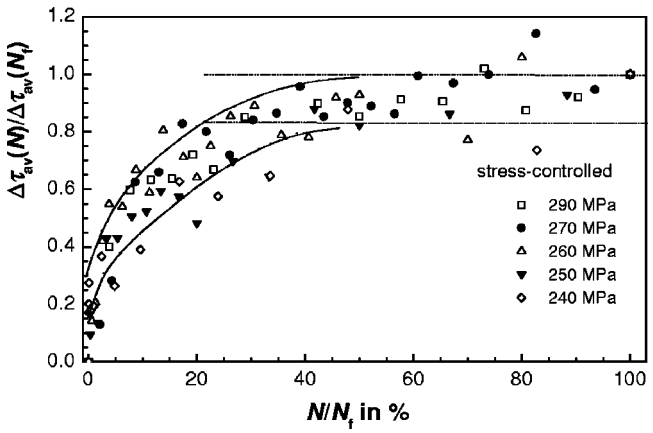

FIG. 7. Evolution of the increase of the average positron lifetime $\Delta\tau_{av}(N) = \tau_{av}(N) - \tau_{av}(0)$ during fatigue life in the stress-controlled experiments (A290, A270, A260, A250, and A240) presented in Fig. 5 normalized to the value at failure $\Delta\tau_{av}(N_f)$. The fatigue life is given by the number of load cycles N normalized to the number of cycles at failure N_f. The eye guides indicate a typical ''bandwidth'' for stress-controlled experiments.

amplitudes between 350 and 400 MPa have been determined from the hysteresis loops for this plastic strain amplitude. The stress amplitudes reached in the strain-controlled experiments in the range of $1 \times 10^{-4} \leqslant \varepsilon_{pl} \leqslant 5 \times 10^{-3}$ were between 212 and about 400 MPa. In Fig. 9 the increase of the average positron lifetime until failure, $\Delta\tau_{av}$, is plotted versus the applied stress amplitude σ. In spite of the scatter, that deserves a closer look later, $\Delta\tau_{av}(N_f)$ increases monotomically with increasing applied stress amplitude σ. The strain-controlled experiments do not exhibit such a tendency. In Fig. 10 $\Delta\tau_{av}(N_f)$ exhibits an appreciable scatter but definitely no dependence on the applied plastic strain amplitude ε_{pl}.

Under plastic strain control the average positron lifetime was increasing from start values between 107 and 132 ps up to values between 139 and 162 ps at failure. The highest

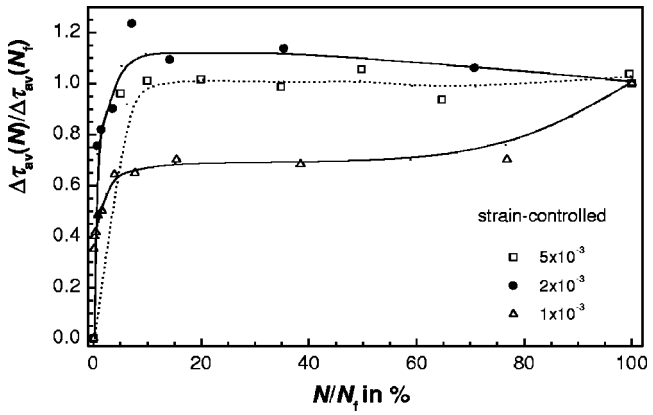

FIG. 8. Evolution of the increase of the average positron lifetime $\Delta\tau_{av}(N) = \tau_{av}(N) - \tau_{av}(0)$ during fatigue life in the strain-controlled experiments (B5E3, A2E3, and D1E3) presented in Fig. 6 normalized to $\Delta\tau_{av}(N_f)$. The fatigue life is given by the number of load cycles N normalized to the number of cycles at failure N_f.

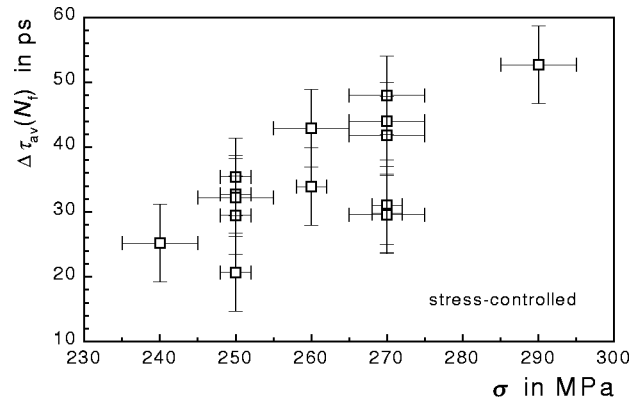

FIG. 9. Increase of the average positron lifetime until failure $\Delta\tau_{av}(N_f)$ in ps vs the applied stress amplitude σ in MPa for all stress-controlled experiments that were continued until failure.

value of $\tau_{av}=162$ ps was registered for $\varepsilon_{pl}=5\times10^{-3}$. In stress-controlled experiments an increase from start values between 111 and 138 ps to average positron lifetimes between 141 and 186 ps was found in spite of larger values for N_f and lower stress levels as compared to those obtained in most of the strain-controlled experiments.

B. Examination of hysteresis loops—deformation work

Figures 11 and 12 present the development of the deformation work w per cycle as a function of the number of fatigue cycles N for some stress and strain-controlled experiments, respectively. The evaluation of the hysteresis loops gives the deformation work in MJ/m^3 per cycle and reaches values of about 2.5 MJ/m^3 and of up to 6 MJ/m^3 for the shown stress- and strain-controlled experiments, respectively. In order to have a more intuitive number, these values have been converted in meV/atom using the lattice constant $a=3.51\times10^{-10}$ m of AISI 316 L stainless steel[87] and $a^3/4$ as the unit cell volume of a fcc crystal structure, which yields 1 MJ/m$^3=6.75\times10^{-2}$ meV/atom. A comparison between

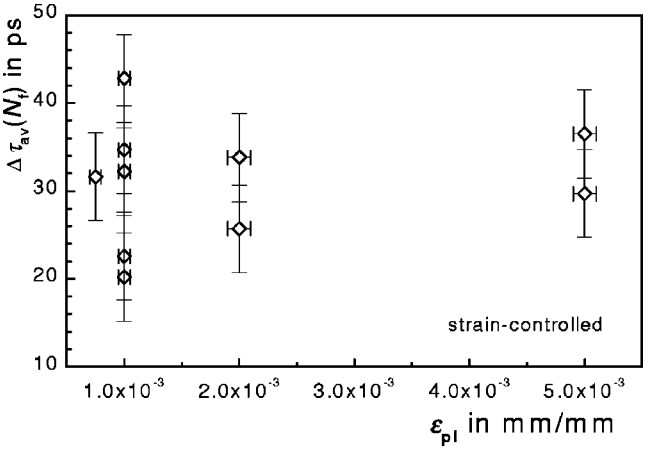

FIG. 10. Increase of the average positron lifetime until failure $\Delta\tau_{av}(N_f)$ in ps vs the applied plastic strain amplitude ε_{pl} in mm/mm for all strain-controlled experiments that were continued until failure.

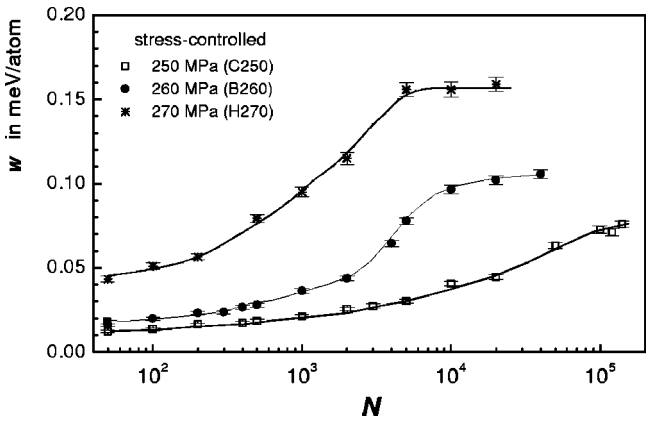

FIG. 11. Evolution of deformation work w in meV/atom as derived from the area of the hysteresis loops for stress-controlled fatigue experiments [C250, B260, and H270 (cf. Table II)].

Figs. 11 and 12 shows the striking difference in the material behavior under the chosen experimental conditions. The stress-controlled experiments (Fig. 11) show a pronounced increase of the deformation work per cycle by a factor of about 4 until failure. In the strain-controlled experiments (Fig. 12) a slight cyclic softening is observed reducing the initial values of the deformation work by about 10%. After 1.000 or, at the latest, 10.000 cycles a plateau is reached indicating cyclic saturation. This indicates that the defect densities are susceptible to fatigue induced changes in stress-controlled experiments for a much longer fraction of the fatigue life than in strain-controlled experiments.

If we plot the average positron lifetime at failure $\tau_{av}(N_f)$ versus the deformation work per fatigue cycle, w, in cyclic saturation for all available experiments, as done in Fig. 13, a gap of about 0.2 meV/atom between the stress-controlled experiment with $\sigma=270$ MPa and strain-controlled experiments carried out at $\varepsilon_{pl}=5\times10^{-3}$ is remarkable. For the stress-controlled experiments the figure indicates a tendency of $\tau_{av}(N_f)$ to increase with increasing deformation work w. If the rather isolated data for $\varepsilon_{pl}=5\times10^{-3}$ ($w\approx0.4$ meV/atom) are considered such a tendency can also be

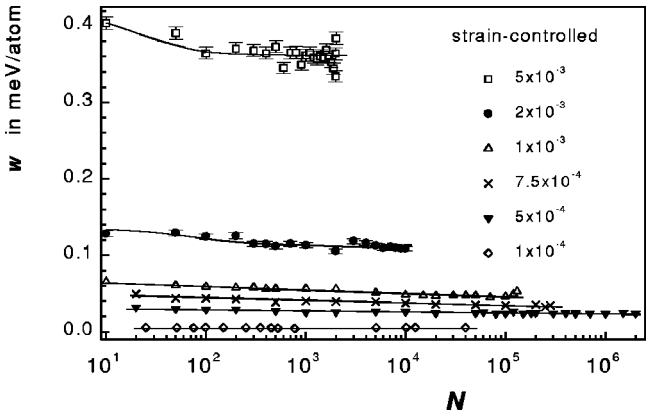

FIG. 12. Evolution of deformation work w in meV/atom as derived from the area of the hysteresis loops for strain-controlled fatigue experiments [B5E3, A2E3, D1E3, B75E4, C5E4, and A1E5 (cf. Table III)].

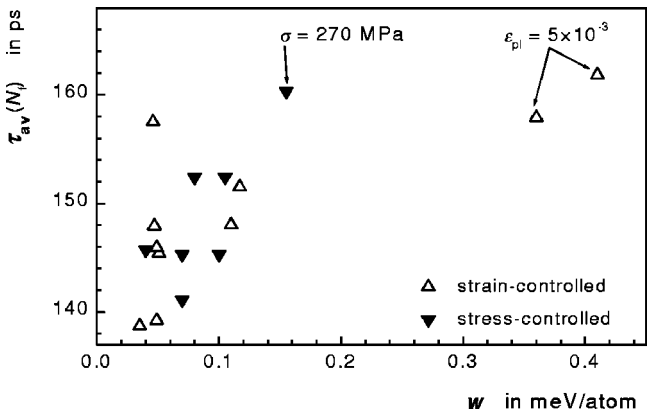

FIG. 13. Average positron lifetime measured after failure $\tau_{av}(N_f)$ in ps vs the deformation work w in meV/atom in cyclic saturation. The gap in w between the stress- and strain-controlled experiments executed with amplitudes of $\sigma = 270$ MPa and $\varepsilon_{pl} = 5 \times 10^{-3}$, respectively, as described in the text is indicated.

derived for plastic strain-controlled experiments. From Fig. 14 it becomes evident that a dependence of $\tau_{av}(N_f)$ on w in cyclic saturation implies also a dependence on fatigue life N_f.

C. Reproducibility of experiments

1. Positron annihilation measurements during fatigue

The different measurement campaigns contributing to the results presented in the present paper were performed with two different specimen geometries on three fatigue systems and with three ^{72}Se/^{72}As positron generators. Whenever the positron generator was replaced in the lifetime spectrometer the adjustments of the nuclear electronics were checked and sometimes slightly modified to optimize performance. The overall reproducibility of the experiments was sufficiently good. However, fatigue of materials—by its nature—is subjected to pronounced experimental scatter. In engineering design safety margins are applied that take into account that the number of fatigue cycles until failure N_f as derived from Wöhler curves may vary by a factor of 3–5.

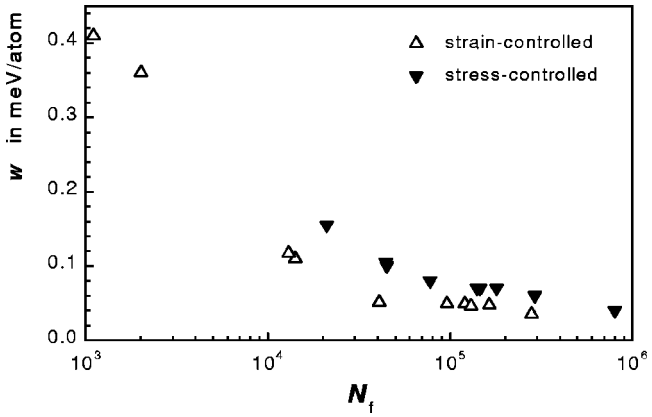

FIG. 14. Relation between deformation energy w in meV/atom and the fatigue life given by the number of load cycles until failure N_f for stress- and strain-controlled experiments.

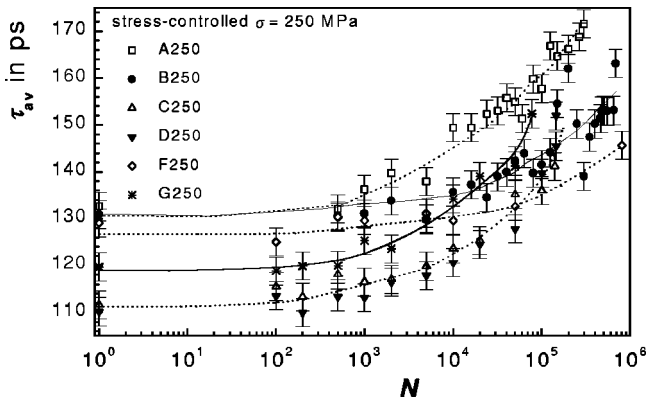

FIG. 15. Evolution of the average positron lifetime τ in ps during stress-controlled fatigue experiments with a stress amplitude of $\sigma = 250$ MPa. Experiments C250 and D250 are represented by one eye guide only.

In spite of the scatter in Fig. 9 a clear tendency of increasing $\Delta\tau(N_f)$ with increasing applied stress amplitude σ can be recognized. However, the scatter could limit the utility of the positron annihilation technique for nondestructive testing especially for a residual lifetime assessment of components. One contribution to the scatter is likely the uncertainty of the manual adjustment of the stress amplitude for the experiments performed on the Instron 1273 system that allowed an accuracy of only ± 5 MPa, whereas the computer controlled MTS systems allowed a reproducibility of the stress amplitude better than ± 2 MPa.

In Figs. 15 and 16 experiments are presented that were carried out with a stress amplitude of 250 MPa. Comparing these figures shows that experiment F250, with the lowest observed increase of the positron lifetime until failure $\Delta\tau_{av}(N_f)$ and the longest observed fatigue life of $N_f = 802.300$, also had the smallest values of the deformation work w. On the other hand, in experiment G250 $\Delta\tau_{av}(N_f)$ is in the range of the other experiments at this stress amplitude. The early failure at $N_f = 77.635$ that has not been predicted by the evolution of the average positron lifetime, however, is reflected in the highest observed deformation work at σ

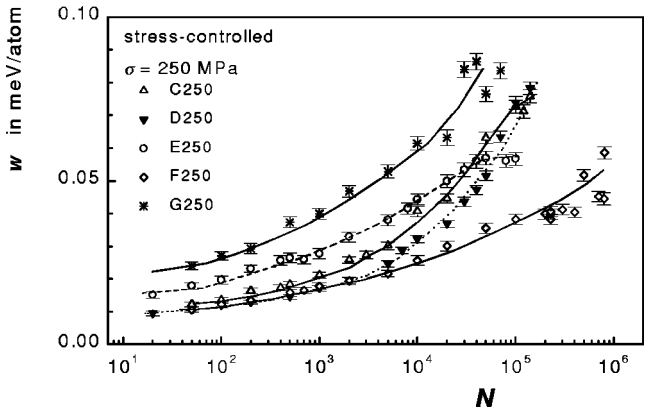

FIG. 16. Evolution of the deformation work w in meV/atom during stress-controlled fatigue experiments with a stress amplitude of $\sigma = 250$ MPa.

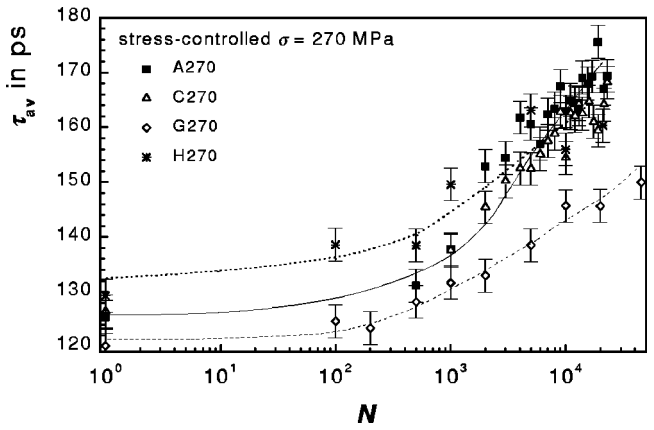

FIG. 17. Evolution of the average positron lifetime τ_{av} in ps during stress-controlled fatigue experiments with a stress amplitude of $\sigma=270$ MPa. The experiments A270 and C270 are represented by one eye guide only.

$=250$ MPa. In experiments C250 and D250 with similar fatigue lives of $N_f=140.226$ and 145.621, respectively, the evolution of $\Delta\tau_{av}$ proceeds rather parallel to that of the deformation work w. The same analysis can be made for $\sigma=270$ MPa on the basis of Figs. 17 and 18. However, for this stress amplitude only two experiments were carried out with strain measurement. Their values for N_f differ by a factor of 2, but $\Delta\tau_{av}(N_f)$ is identical within the experimental error. Also in this case the specimen with the shorter fatigue life has a significantly higher deformation work w and the increase of $\Delta\tau_{av}(N)$ proceeds faster, though ending at the same level for $\Delta\tau_{av}(N_f)$. In most cases a different evolution of the average positron lifetime is related to a significantly different fatigue life N_f.

Figures 19 and 20 show the evolution of the average positron lifetime and of the deformation work for the five experiments conducted at a plastic strain amplitude of $\varepsilon_{pl}=1\times10^{-3}$. The scatter is less pronounced than in stress-controlled experiments. One eye guide describes the evolution sufficiently for the complete series of experiments. In both figures a saturationlike behavior after about 10% of fatigue life can be recognized. The good reproducibility may

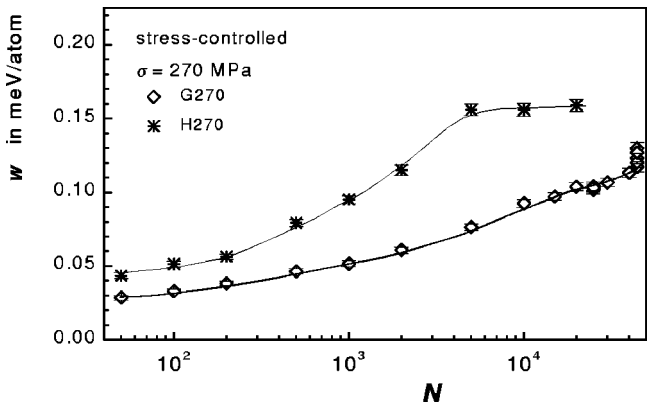

FIG. 18. Evolution of the deformation work w in meV/atom during stress-controlled fatigue experiments with a stress amplitude of $\sigma=270$ MPa.

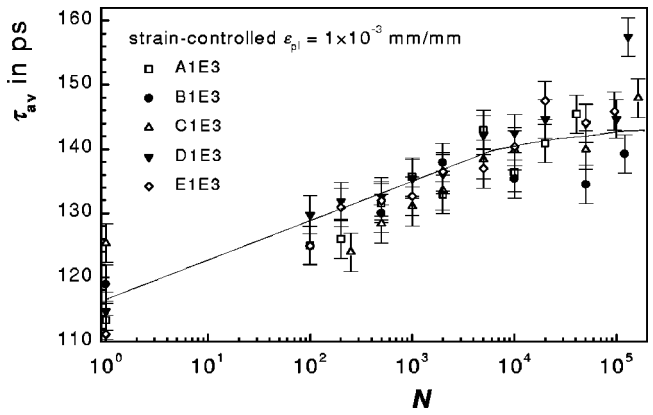

FIG. 19. Evolution of the average positron lifetime τ_{av} in ps during strain-controlled fatigue experiments with a plastic strain amplitude of $\varepsilon_{pl}=1\times10^{-3}$ mm/mm. The eye guide indicates the saturation of τ_{av} after about 10% lifetime.

reflect the better control on the dislocation motion and consequently the evolution of the fatigue microstructure in strain-controlled experiments as indicated by Eq. (1). The initial scatter of $\tau_{av}(N=0)$ is practically wiped out within the first 500 deformation cycles.

2. Measurements in different points on the specimen surface

In order to check a possible variation of average positron lifetime due to the location of the measurement site on the specimen surface, on some specimens the initial measurements have been repeated varying the position of the source–detector assembly along the gauge length in steps of about 5 mm. Additionally some specimens have been rotated and the measurements repeated (180° for B2E3, 120° and 240° for B4E5). The variation of the measured average positron lifetimes was always within a range of at maximum ±3 ps.

The experiment with specimen A1E3 ($\varepsilon_{pl}=1\times10^{-3}$) has been automatically stopped by the fatigue machine after detecting a crack on the gauge length. The crack was visible on the specimen surface to the naked eye and penetrated half

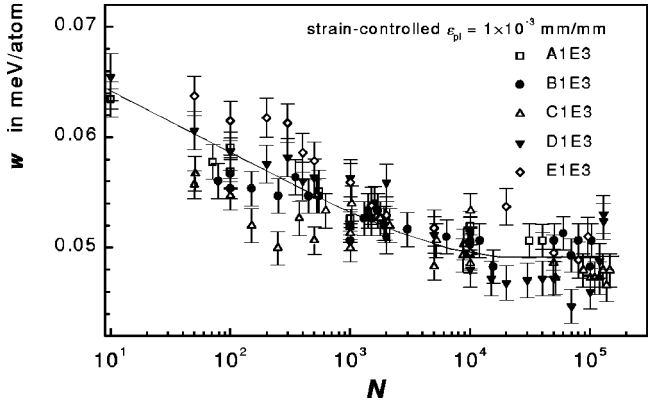

FIG. 20. Evolution of the deformation work w in meV/atom during strain-controlled fatigue experiments with a plastic strain amplitude of $\varepsilon_{pl}=1\times10^{-3}$ mm/mm. A saturationlike behavior of w can be recognized after about 10% lifetime as observed for τ_{av} in Fig. 19.

into the specimen diameter. In view of the penetration depth and the area irradiated by the positrons, the crack tip itself has not been reached by the positrons. $\tau_{av}(N_f)$ has been determined as 145 ps. Then the specimen was adjusted in a way to measure just on the opposite site of the crack. $\tau_{av}=148$ ps has been obtained that agrees well with $\tau_{av}(N_f)=145$ ps. Then a measurement 10 mm above the plane of crack propagation was performed without rotating the specimen and a value of $\tau_{av}=165$ ps has been obtained. Rotating the specimen by 180° and now measuring 10 mm above the open crack yielded a value of $\tau_{av}=142$ ps, that is still compatible with the 145 ps measured as $\tau_{av}(N_f)$. This shows that the values for $\tau_{av}(N_f)$ are more uncertain than those taken before failure. We interpret this result as an excessive straining of the material on the side opposed to the crack in the last few deformation cycles before failure. The crack itself does not allow the load to pass in the material above and below the already separated parts of specimen. On the crack plane itself, in front of the propagating crack deformation energy is consumed by creating a new crack surface rather than by a plastic straining of the material accessible by positrons. Consequently, in the material that could be reached by positrons on the crack-opposed side of the crack propagation plane a value of $\tau_{av}=148$ ps was preserved.

In view of the uncertainty introduced by the fracture process on the values for $\tau_{av}(N_f)$ we checked all data obtained so far on extraordinary jumps in the evolution of $\tau_{av}(N)$ between $\tau_{av}(N_f)$ and the last value recorded before failure. Experiment D1E3, presented in Figs. 4 and 6 (symbol: $\triangle$), was the only experiment that gave some indication for such an event. However, D1E3 does not affect any conclusions we draw from our experiments. We did not increase the error marks for the positron lifetime data at failure, because the error of ± 3 ps for τ_{av} is based on measurement statistics and on the reproducibility of measurements and data evaluation and therefore well defined. There is no argument to define a meaningful error margin in the case of such exceptional error sources.

IV. DISCUSSION

A. Comparison with other experimental investigations

The main scope of the present work was to examine the evolution of the average positron lifetime during stress- and strain-controlled fatigue experiments in order to assess the reproducibility and the predictive power of positron lifetime measurements for nondestructive testing purposes. There was no need to prove the principal sensitivity of positron annihilation to fatigue damage. This was already done in the past for many different materials in different types of experiments: e.g. for pure copper by Alexopoulos and Byrne,[54] and Kupca *et al.*,[88] for nickel by Grobstein *et al.*[55] for nickel and Ni-Co alloy by Lynn *et al.*,[56] for Fe-0.5-wt %Si by Kuramoto *et al.*,[89] for mild steel by Karjalainen *et al.*,[90] for stainless steel AISI 316 by Gauster *et al.*,[57] and more recently for AISI 304 by Hartley *et al.*[58] and by Bennewitz *et al.*[91] for the stainless steel X6CrNiTi18-10 and the carbon steel C45E.

The most complete work focused on nondestructive testing was recently published on positron annihilation experiments on stainless steel AISI 316 L by Kawaguchi and different co-workers.[69,70,72] These authors reported on positron-lifetime measurements and annihilation line shape analysis in stress-controlled experiments in the range $200\ \text{MPa} \leqslant \sigma \leqslant 250$ MPa and on strain-controlled experiments in the range $2.5\times10^{-3} \leqslant \varepsilon_{tot} \leqslant 3.1\times10^{-3}$. Unfortunately only the publication of Kawaguchi and Shirai[69] is in English. References 70 and 72 are in Japanese but with English figure captions.

In their publication Kawaguchi and Shirai[69] report the results of positron lifetime measurements and positron annihilation line shape analysis for stress- and strain-controlled tension-compression fatigue at amplitudes of $\sigma=220$ MPa and $\varepsilon_{tot}=3.1\times10^{-3}$, respectively. In their strain-controlled experiments the total strain has been controlled. In doing so the corresponding plastic strain value required for a comparison with the present experiments is (i) smaller ($\varepsilon_{pl}<\varepsilon_{tot}$) and (ii) not constant throughout the experiments which may result in a different microstructure evolution.

Kawaguchi and Shirai[69] reported that they used three specimens to determine the typical fatigue life N_f for $\sigma=220$ MPa and $\varepsilon_{tot}=3.1\times10^{-3}$. Further specimens were cyclically deformed to 0.1 , 1, 10, 25, 50, and 100% of this value. This presents an important difference to the present work because the positron annihilation measurements to follow the evolution of fatigue damage were performed on different specimens deformed to a different stage of fatigue life. This introduces an uncertainty concerning the real percentage of fatigue life. In view of the possible scatter of fatigue life as indicated in Fig. 2, we assume that this might be the reason that no further data are available between 50 and 100% of fatigue life where the uncertainty of N_f could cause *early* failure. Moreover, Kawaguchi and Shirai[69] determined a fatigue life of $N_f=357.000$ for their material at a stress amplitude of 220 MPa. The material used for the present report exhibits a lifetime of $N_f>10^7$ for $\sigma=220$ MPa, and $N_f=357.000$ could be expected for $\sigma\approx250$ MPa. Hence, the AISI 316 L used by Kawaguchi and Shirai[69] was in a microstructure state that made it more prone to fatigue failure than the material used for the experiments presented here. The reasons for this could be a slightly different chemical composition, a longer thermal pretreatment, and a different quenching rate achieved in the tube material as compared to the plates from which our specimens were prepared.

In spite of the experimental differences described above Kawaguchi and Shirai[69] confirmed one of the present major findings, i.e., that the evolution of average positron lifetime proceeds faster in strain-controlled experiments than under stress control. The different experimental method applied by Kawaguchi and Shirai allowed these authors however to carry out TEM examinations of the microstructure evolution in the same specimens examined before by positron annihilation. But the authors did not quote values for the development of the average dislocation density. Such quantitative data are indeed very difficult to obtain in view of the inhomogeneous dislocation distribution with alternating dislocation-poor and -dense regions. If no weak beam experiments are performed, TEM fails to give reliable data on the

dislocation dense regions where dislocation densities of some 10^{15}–10^{17} m^{-2} can be reached.

A very important result in view of possible future applications was obtained by plotting τ_{av} versus the parameter S that characterizes the annihilation line shape for specimens examined both by positron-lifetime measurements and annihilation line shape analysis. Kawaguchi and Shirai[69] convincingly demonstrated that the evolution of the average positron lifetime τ_{av} and that of the S parameter are equivalent.

Hartley *et al.*[58] examined two batches of stainless steel AISI 304 that differed in their carbon content (0.056 at% and 0.014 at%). Like Kawaguchi and Shirai[69] they determined an average fatigue life under the applied fatigue conditions (strain control, $\varepsilon_{tot}=6.6\times10^{-3}$) and then cycled different specimens up to different stages in fatigue life. The positron lifetime was measured using a 2.5-MeV positron beam of Lawrence Livermore National Laboratory and the spectra were decomposed in short ($\approx$100 ps) and long ($\approx$210 ps) lifetime components. The long component was found to saturate after about 10% of fatigue life at an intensity of around 70–80 %.

An early saturation of average positron lifetime in fatigue life has also been reported in investigations on nickel and Ni-66.5%Co alloy by Lynn *et al.*[56] These experiments were carried out in constant maximum stress cantilever bending. Two identically deformed specimens were prepared in order to measure nondestructively the average positron lifetime in various stages of fatigue life by sandwiching a ^{22}Na source between them. Bending fatigue, however, introduces a gradient of the stress amplitude from a maximum value at the surface to zero on the neutral line in the center of the specimen. Although the bending stress has been controlled in this case the positrons probe a volume subjected to different local stress and strain amplitudes. Therefore, the results are difficult to compare with the present ones and those discussed so far. The same experimental method has been applied by Karjalainen *et al.*[90] on mild steel (Fe-0.16%C-0.45%Mn) but a more gradual increase of the average positron lifetime has been obtained during fatigue life.

In fatigue of copper, applying the method described in the preceding paragraph, Alexopoulos and Byrne[54] found differences in the saturation behavior that strongly depend on the initial state of the specimens. Annealing the cold rolled cantilever bending specimens at temperatures of 366.3, 533, and 672 K, and subsequent cyclic bending at stresses of 1.3 times the respective yield stress, produced a saturationlike behavior, a fast saturation, and a more gradual increase of the average positron lifetime, respectively. This underlines the importance of precise knowledge of the initial state of the material.

B. Predictive power and reproducibility

Ideally, when a nondestructive testing method is applied one wishes to answer the question of what percentage of the lifetime the component or specimen is arrived at. A practical handicap, which is avoided in laboratory experiments, is that often the initial state has not been characterized at all, or by using a different method. But in the present case, different loading conditions can yield the same values for the measured parameter after a different number of load cycles. This means that at least a reasonable assumption about the expected load amplitude or on the number of already applied load cycles is required to complete the task. A necessary condition is the reproducibility of the results under nominally identical fatigue conditions and initial microstructure.

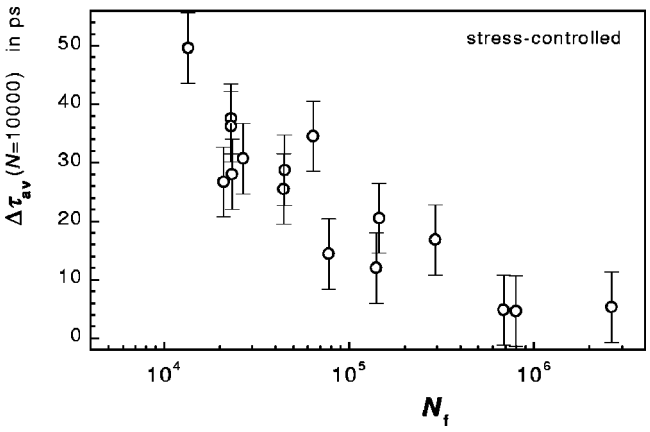

FIG. 21. Relation between the increase of the average positron lifetime $\Delta\tau_{av}(10000)$ measured after the first 10.000 load cycles and the fatigue life given by the number of cycles until failure N_f in stress-controlled experiments.

It has already been shown in Figs. 7 and 9 that the increase of the mean positron lifetime until failure depends on the applied stress amplitude and that this value is practically reached after 40% fatigue life. In Fig. 21 the increase of the mean positron lifetime measured after 10.000 load cycles is presented versus the fatigue life. The shape of the curve obtained closely resembles the Wöhler curve used for design purposes. For most stress amplitudes 10.000 cycles are quite early in fatigue life N_f. Hence, with a precise estimate of fatigue cycles N an early conclusion on the obtainable N_f appears feasible. This is exactly the information needed for a residual lifetime assessment; however, the absolute value of N_f exhibits a large scatter the smaller the applied stress amplitude.

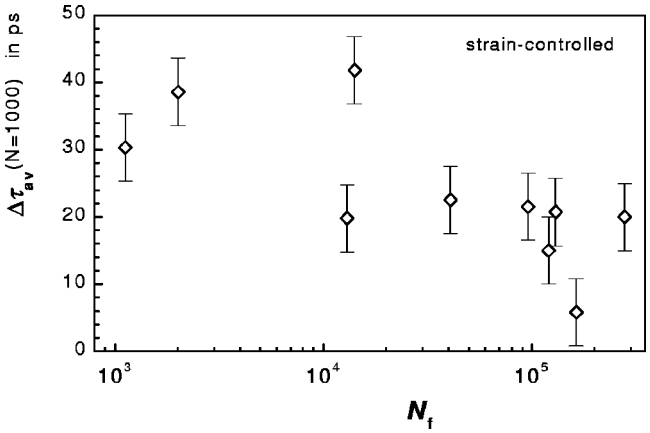

FIG. 22. Relation between the increase of the mean positron lifetime $\Delta\tau_{av}(1000)$ measured after the first 1.000 load cycles and the fatigue life given by the number of cycles until failure N_f in strain-controlled experiments.

In strain-controlled experiments the predictive power is much more limited since $\Delta\tau_{av}(N_f)$ at failure does not depend on ε_{pl}. Also the information that can be obtained from Fig. 22 presenting $\Delta\tau_{av}$ after 1.000 load cycles versus the fatigue life, is only rough, though it might be improved by a better statistics of the positron lifetime spectra. However, in practical applications components have to resist a certain value of alternating maximum stress and strain control is not as important as in fatigue research. On the other hand, in most practical cases, loading occurs with a statistical distribution of stress and stress rate and often with a mean stress unequal to zero, i.e., $\sigma_{min}/\sigma_{max} \neq -1$. Therefore, the aspect of loading with stress spectra and mean stress deserves special attention in future experiments.

C. Defects in dynamic equilibrium

Positron annihilation is highly sensitive to vacancylike defects. However, its capability to distinguish between different kinds of defects is very limited if their specific positron lifetimes are similar. A reliable discrimination between positron traps that differ in their positron lifetime by 50 ps requires at least 3×10^6 coincidence events in the spectra to be analyzed.[86] On the other hand, fatigued metals provide a confusing variety of positron trapping sites that differ appreciably by their positron binding energy but most of the relevant positron traps are assumed to have their positron lifetimes within a range of typically 30–40 ps.[19,31] In such a case not even the number of components for a decomposition of the spectra is clear, and choosing the wrong number will lead to unphysical results for the lifetimes as well for the corresponding intensities. The present study examines the possibility of an engineering application of positron annihilation that avoids this risk, confining itself to analyze the average positron lifetime.

Moreover the evolution of a fatigue microstructure is a dynamic process and consequently the evolution of the densities of various types of possible positron traps is very complex. TEM and electrical resistivity measurements provide evidence for the existence of a state of cyclic saturation in which the concentration of dislocations and atomic defects is kept constant by a dynamical equilibrium between the production and annihilation of dislocations and atomic defects, respectively. It would be useful if positron annihilation could reveal even tiny differences, maybe changes in the configuration of defect clusters, that could be used as an *internal clock* for fatigue life beyond the saturation of the average positron lifetime.

Since positron annihilation studies on fatigue so far never reflected on the dynamic nature of cyclic saturation, the following examples illustrate the turnover of dislocations and atomic defects. In tensile deformation, the stored energy has been precisely determined by deformation calorimetry during tensile deformation of copper single crystals by Rönnpagel and Schwink, and it was found to be about 11% of the deformation work in region II of the tensile stress-strain curve.[92] In 1974 an overview on the stored energy of cold work was given by Bever *et al.*[93] The data collection of Bever *et al.*[93] contains only a few push-pull fatigue data and no experimental data could be found after 1974. The stored energy is reported as about 8 meV/atom. No data are given for the fraction of stored to expanded energy. This fraction depends strongly on the stage of the fatigue life. In cyclic saturation the whole deformation energy is dissipated and the stored energy drops to zero[94] because the densities and the spatial distribution of defects remain constant on a length scale of several micrometers. This conclusion is well supported by a long series of TEM studies during fatigue of various materials,[32,95] showing a constant density of dislocations in cyclic saturation, and by accompanying measurements of the electrical resistivity indicating that also the concentration of atomic defects saturates, however a little later in fatigue life.[42,53]

The amount of dislocation production and annihilation in cyclic saturation has been illustrated by Seeger and Frank:[94] ϱ_a is the dislocation density annihilated and recreated within one deformation cycle and Gb^2 the energy per unit length of a dislocation with a Burgers vector b in a material with a shear modulus G; then ϱ_a can be calculated from

$$\oint \sigma \mathrm{d}\varepsilon_{pl} = \frac{1}{2}\varrho_a G b^2. \tag{4}$$

With a typical value of 0.1 meV/atom (1.48 MJ/m^3) for the deformation work in our experiments and a modulus of a primary Burgers vector of type $\langle 110\rangle$ of $b=2.48\times10^{-10}$ m and a shear modulus of $G=74.8$ GPa (Ref. 78) in each fatigue cycle a dislocation density of 6.4×10^{14} m^{-2} is annihilated and recreated. This corresponds roughly to the complete dislocation content of the material. This result illustrates the nearly complete irreversibility of cyclic deformation on a microscopic level in the sense that the dislocations carrying plastic deformation in the tensile half-cycle are not those carrying plastic deformation in the following compression half-cycle.[96,97]

A major annihilation mechanism for dislocations is the collapse of narrow edge dislocation dipoles.[33,35] This gives rise to the formation of atomic defects which are themselves in a dynamic equilibrium between production and annihilation. There are various possibilities of elastic interaction between atomic defects and dislocations. Moving dislocations can segment atomic defect clusters and pick up atomic defects, thereby creating jogs on dislocation lines.[45] The repeated pickup of atomic defects can move jogs along a dislocation line and cause the dislocation to climb. In this way atomic defects can efficiently be eliminated and an equilibrium concentration is kept.

In the literature sometimes reference is made to the model of Saada[48] that allows one to estimate the concentration of atomic defects in ranges I and II of the stress-strain curve of a tensile test. The simple model of Saada is, however, not applicable to fatigue, perhaps with the exception of the first few cycles of a well annealed specimen, where dislocation distribution is still homogeneous and the dislocation density is low and far from saturation. If we follow Dìaz *et al.*[44] and apply Saada's model on the first quarter cycle of a strain-controlled experiment with $\varepsilon_{pl}=1\times10^{-3}$, we get, for the vacancy concentration

$$C_V = \frac{1}{2}\frac{\beta}{G}\int_0^{1\times10^{-3}} \sigma d\varepsilon_{pl}, \quad (5)$$

a value of about 6×10^{-8} vacancies per atom. Here we used a shear modulus of $G=74.8$ GPa (Ref. 78) and the numeric factor $\beta=0.06$ as derived by van den Beukel.[98] If we now return to our hysteresis loops and the measured deformation work, we will see that this is a fatally reasonable number derived from a non-applicable model. In Fig. 20 the deformation work for the experiment with $\varepsilon_{pl}=1\times10^{-3}$ decreases slightly from about 0.6 meV/atom during the first 100 cycles to a rather constant value of 0.55 meV/atom reached after about 10 000 cycles. We assume that the 0.55 meV/atom is completely dissipated into heat and that the difference of the 0.05 meV/atom is the stored energy per cycle within the first cycles. We further assume that 99% of this amount is initially stored as dislocations and only 1% as atomic defects (0.5% as vacancies and 0.5% as interstitials). Taking into account the formation enthalpy of a vacancy in stainless steel[80] of $H_V^F=1.61$ eV the vacancy concentration could increase by 1.55×10^{-7} per atom in one load cycle. With these rough but not unreasonable assumptions we reach the same order than with the Saada model but without exceeding its limits of validity.[48,99] We have to be aware that the amount of stored energy drops to zero until cyclic saturation is reached; however, with the assumed average value of 0.05 meV/atom within the first 1.000 cycles a vacancy concentration of $1.55\times10^{-7}\times1000=1.55\times10^{-4}$ could be obtained that would provoke saturation trapping of positrons, homogeneous vacancy distribution provided. If computer simulations becomes available that could predict the evolution of dislocation density and of the densities of atomic defects in the lattice and of jogs on dislocation lines during fatigue cycling, starting from grown-in dislocations after careful annealing, it appears feasible that such simulations could be checked by TEM in combination with positron annihilation and measurements of electrical resistivity.

D. Inhomogeneous distribution of defects

In face centered cubic metals such as austenitic stainless steels plastic strain may become localized in persistent slip bands (PSBs). In such cases of strain localization the dynamic equilibrium between defect production and annihilation described in the preceding section is valid only in the volume fraction occupied by PSBs. These PSBs are embedded in a so-called matrix structure that deforms mainly elastically under applied cyclic loading. According to the model of Essmann, Gössele, and Mughrabi[45] a diffusion flux of vacancies can be expected from the PSB regions into nearly unstrained matrix material. In such border regions between PSBs and matrix vacancy agglomerates may be formed that are protected from being segmented by moving dislocations since the small plastic strain amplitudes in the matrix regions can be accomplished by a flipflop motion of screw dislocations in the dislocation poor channels that separate veins with high dislocation density.[45] Therefore, a significant concentration of spherical vacancy clusters could exist in a border stripe between PSBs and the matrix. Since on the matrix side no significant dislocation motion takes place, spherical vacancy clusters should be stable at least as long as they do not collapse into small sessile dislocation loops.

In view of the diffusion length of thermalized positrons under the present conditions that can be estimated to about 0.25 μm (Ref. 17) and the inhomogeneous distribution of dislocations in patterns of alternating dense and poor regions with a typical separation of 1–2 μm, not all positrons will annihilate in the same environment. Therefore, the question will be if spherical vacancy agglomerates that may exist in a small volume fraction of the material will obtain a sufficient statistical weight to be retrievable may be as a long-lived lifetime component in positron lifetime measurements.

Consequently, attempts to improve the spatial resolution of positron annihilation by developing positron ''microbeams''[102] or positron ''microscopes''[103] are very promising assets for basic fatigue studies and in support of nondestructive testing. Considerations of statistical weight show also that positron trapping in grain boundaries can be neglected in the present case in view of the grain sizes around 40–50 μm.

E. Positron traps and trapping models

The interpretation of the present experiments is entirely based on the average positron lifetime due to the applied methods for background correction and in order to avoid misinterpretations introduced by a lack of knowledge concerning the number of components required for a physically meaningful decomposition of the positron lifetime spectra. However, a positron annihilation study after isochronal annealing of slabs prepared from the same material batch and compressed to 10% and 20% thickness reduction[67] gave no indication of other positron traps than single vacancies. The conclusion of this study agrees well with a fatigue study of stainless steel 316 L by Gauster *et al.*,[57] who found that in stainless steel 316 positrons are primarily trapped at lattice vacancies produced by cold work.

Nevertheless, a parameter that changes significantly during the second half of the fatigue life would be useful to bridge the gap between early detection of fatigue damage by positron annihilation shown in the present paper and the sensitivity range of various already established techniques. More coincidence events would be required for this purpose, and a sounder knowledge on the nature of the trapping sites is needed.

Various alternative trapping sites may exist that may not be detectable at room temperature or that may have a low statistical weight. Dislocation lines as shallow traps may facilitate positron trapping into vacancies trapped in the elastic strain field around a dislocation, without being directly visible at room temperature due to thermal detrapping. Doyama and Cotterill[25] suggested jogs on dislocation lines as trapping sites. Theoretical calculations by Häkkinen *et al.*[19] showed at least for aluminum that such jogs on $[1\bar{1}2]$ edge dislocations (line direction) are stable traps at room temperature, but they exhibit a positron lifetime of 224 ps that makes them difficult to distinguish from annihilation in a lattice vacancy (252 ps) and in a vacancy trapped in the compression zone around an

edge dislocation in Al (225 ps).[19] Moreover, with a stacking fault energy of about 28 mJ/m^2 (Refs. 63, 100) a splitting up of dislocations into partial dislocations has to be taken into account, which are separated by a stacking fault ribbon. The open volume along the partial dislocations is even smaller but the effect of vacancies in the stacking fault ribbon has to be considered in this case.

Evidence of the existence of vacancy clusters in fatigued metals has been published by various authors. Contrast phenomena in TEM investigations on fatigued copper single crystals have been interpreted as vacancy clusters with a diameter of up to 4 nm by Piqueras *et al.*[43] and others.[23,44] Grobstein *et al.*[55] performed measurements of electrical resistivity and positron annihilation during fatigue of nickel. These authors showed a decrease of the positron lifetime in vacancy clusters during fatigue that has been explained with a decreasing size of the clusters.[55] This result contrasts, however, with earlier investigations on fatigue of nickel examined by positron annihilation by Gauster *et al.*[57] giving no indication of vacancy clusters. Corbel *et al.*[101] from calculations of the electron density, derived that the positron lifetime depends not only on the number of vacancies in the cluster but also on their configuration. In a spherical vacancy cluster in gold positron lifetime increases from about 200 ps (single vacancy) to nearly 400 ps with 15 vacancies. But if relaxation occurs, the positron lifetime may decrease appreciably.[101] This holds even more when vacancies are arranged in a vacancy (dislocation) loop on a close packed plane. Häkkinen *et al.*[19] calculated the positron lifetime in a vacancy loop in aluminum and obtained a value of 191 ps whereas the lifetime in a single vacancy was calculated with 252 ps. Moreover, the binding energy drops from 2 eV in a single vacancy to 0.4 eV in such a loop.[19] Therefore, even in a high concentration of vacancies it is not a priori clear if a long-lived positron lifetime component can be expected.

Due to the potential of positron annihilation for nondestructive testing it is worth to undertake some further efforts to clarify these problems. Methods that combine a high spatial resolution[102,103] and the possibility to accurately measure the positron lifetime[103] seem to be most appropriate.

V. CONCLUSIONS

The results presented demonstrate that positron annihilation can be developed into a highly sensitive tool for the nondestructive testing of fatigue damage in stainless steel AISI 316 L. The major findings agree well with those of Kawaguchi and different co-workers.[69,70,72] Moreover, an analysis of the reproducibility of the measurements and the differences between stress- and strain-controlled measurements shows that significant experimental deviations under nominally identical conditions can be understood when further parameters like deformation work are taken into consideration. This indicates that positron annihilation is sensitive to effects of initial microstructure and material history that affect the density evolution of positron traps. With a known initial material state, measurements of the average positron lifetime have a predictive power that can be used for residual lifetime estimates. Following such an empiric approach the next steps have to consider experiments with a more complex fatigue history experimentally realized by fatigue sequences with different stress amplitudes and nonzero mean stress.

More sophisticated applications of positron annihilation in nondestructive testing require a better understanding of the evolution of fatigue microstructure, giving rise to the coexistence of a confusing variety of positron trapping sites in a complex spatial distribution. Due to the dimension and nature of positron trapping sites and the lack of alternative methods with sufficient sensitivity and specificity, modeling fatigue dislocation structures with special emphasis on coproduced jogs, vacancies, and vacancy clusters appears to be one of the very view promising ways. Accompanying temperature dependent positron annihilation measurements starting from very low temperatures with excellent statistics on very pure metals and the application of methods that allow a spatial resolution of positron annihilation in the micron range could then better elucidate possible gains from decomposition of annihilation spectra into lifetime components. Though probably not feasible for nondestructive testing purposes in practice, such attempts could mutually foster progress in fatigue research and in practical applications of positron annihilation.

It is likely that a better understanding of fatigue processes and of positron-defect interaction in fatigued metals could indicate parameters or combinations of parameters more adequate for nondestructive testing and residual lifetime assessment than the average positron lifetime used in the present work by providing a more precise ''internal clock for fatigue life'' of the material.

ACKNOWLEDGMENTS

The authors would like to thank the referee for valuable and very helpful comments on the mauscript, Dipl.-Phys. Sabine Hansen-Ilzhöfer, and Dr. Ing. Achim Ilzhöfer for their support in the performance of the fatigue experiments in the start-up phase of this research as well as Sergio Colpo for taking care of the fatigue machines.

[1] J.D. Achenbach, Int. J. Solids Struct. **37**, 13 (2000).
[2] G. Dobman, N. Meyendorf, and E. Schneider, Nucl. Eng. Des. **171**, 95 (1997).
[3] I.Yu. Dekhtyar, D.A. Levina, and V.S. Mikhalenkow, Dokl. Akad. Nauk. **156**, 795 (1964) [Sov. Phys. Dokl. **9**, 492 (1964)].
[4] S. Berko and J.C. Erskine, Phys. Rev. Lett. **19**, 307 (1967).
[5] J.G. Byrne, in *Dislocations in Solids*, edited by F.R.N. Nabarro (North-Holland, Amsterdam, 1983), Vol. 6, p. 263.
[6] R.N. West, Adv. Phys. **XXII**, 263 (1973).
[7] R.M. Nieminen and M.J. Manninen, in *Positrons in Solids*,

Springer Series *Topics in Current Physics*, edited by P. Hautojärvi (Springer-Verlag, Berlin, 1979), p. 143.
[8] P.J. Schulz and K.G. Lynn, Rev. Mod. Phys. **60**, 701 (1988).
[9] M.J. Puska and R.M. Nieminen, Rev. Mod. Phys. **66**, 841 (1994).
[10] A. Seeger, Philos. Mag. **46**, 1194 (1955).
[11] P.B. Hirsch and D.H. Warrington, Philos. Mag. **6**, 735 (1961).
[12] J.P. Hirth and J. Lothe, *Theory of Dislocations*, 2nd ed. (Krieger, Malabar, FL, 1982).
[13] E. Hashimoto, J. Phys. Soc. Jpn. **62**, 552 (1993).
[14] G. Trumpy, Phys. Lett. A **192**, 261 (1994).
[15] E. Hashimoto, M. Iwami, and Y. Ueda, J. Phys.: Condens. Matter **6**, 1611 (1994).
[16] K. Petersen, I.A. Repin, and G. Trumpy, J. Phys.: Condens. Matter **8**, 2815 (1996).
[17] T. Wider, S. Hansen, U. Holzwarth, and K. Maier, Phys. Rev. B **57**, 5126 (1998).
[18] T. Wider, K. Maier, and U. Holzwarth, Phys. Rev. B **60**, 179 (1999).
[19] H. Häkkinen, S. Mäkinen, and M. Manninen, Phys. Rev. B **41**, 12441 (1990).
[20] Y. Kamimura, T. Tsutsumi, and E. Kuramoto, Phys. Rev. B **52**, 879 (1995).
[21] Y. Kamimura, T. Tsutsumi, and E. Kuramoto, J. Phys. Soc. Jpn. **66**, 3090 (1997).
[22] Y.-K. Park, J.T. Waber, M. Meshii, C.L. Snead, Jr., and C.G. Park, Phys. Rev. B **34**, 823 (1986).
[23] B.T.A. McKee, S. Saimoto, A.T. Stewart, and M.J. Stott, Can. J. Phys. **52**, 759 (1974).
[24] C. Dauwe, M. Dorikens, L. Dorikens-Vanpraet, and D. Seegers, J. Appl. Phys. **5**, 117 (1974).
[25] M. Doyama and R.M. Cotterill, in *Proceedings of the 5th International Conference on Positron Annihilation*, edited by R.R. Hasiguti and F. Fujiwara (Japan Institute of Metals, Sendai, 1979), p. 89.
[26] S. Dannefaer, D.P. Kerr, S. Kupca, B.G. Hogg, J.U. Madsen, and R.M. Cotterill, Can. J. Phys. **58**, 270 (1980).
[27] M.L. Johnson, S.F. Saterlie, and J.G. Byrne, Metall. Trans. A **9**, 841 (1978).
[28] C. Hidalgo, G. González-Doncel, and S. Linderoth, Phys. Rev. B **45**, 7017 (1992).
[29] C. Hidalgo and S. Linderoth, J. Phys. F: Met. Phys. **18**, L263 (1988).
[30] B. Bergersen and T. McMullen, Solid State Commun. **24**, 421 (1977).
[31] L.C. Smedskjaer, M. Manninen, and M.J. Fluss, J. Phys. F: Met. Phys. **10**, 2237 (1980).
[32] S. Suresh, *Fatigue of Materials*, 2nd ed. (Cambridge University Press, Cambridge, 1998).
[33] U. Essmann and H. Mughrabi, Philos. Mag. Lett. **40**, 731 (1979).
[34] D. Kuhlmann-Wilsdorf and C. Laird, Mater. Sci. Eng. **27**, 137 (1977).
[35] H. Mughrabi, F. Ackermann and K. Hertz, in *Fatigue Mechanisms*, edited by J.T. Fong (American Society for Testing of Materials, Philadelphia, 1979), Vol. 675, p. 69.
[36] L.M. Brown, in *Dislocation Modelling of Physical Systems*, edited by M.F. Ashby, R. Bullough, C.S. Hartley, and J.P. Hirth (Pergamon Press, Oxford, 1981), p. 51.
[37] H. Mughrabi, in *Continuum Models of Discrete Systems*, edited by O. Brulin and R.K.T. Hsieh (North-Holland, Amsterdam, 1981), p. 242.
[38] C. Laird, in *Dislocations in Solids* (Ref. 5), p. 57.
[39] C. Laird, P. Charsley, and H. Mughrabi, Mater. Sci. Eng. **81**, 433 (1986).
[40] Z.S. Basinski and S.J. Basinski, Prog. Mater. Sci. **36**, 89 (1992).
[41] J.G. Antonopoulos and A.T. Winter, Philos. Mag. **33**, 87 (1976).
[42] Z.S. Basinski and S.J. Basinski, Acta Metall. **37**, 3275 (1989).
[43] J. Piqueras, J.C. Grosskreutz, and W. Frank, Phys. Status Solidi A **11**, 567 (1972).
[44] L. Diaz, R. Pareja, M.A. Pedrosa, and R. Gonzalez, Phys. Status Solidi A **92**, 159 (1985).
[45] U. Essmann, U. Gössele, and H. Mughrabi, Philos. Mag. **44**, 405 (1981).
[46] P.O. Kettunen, T. Lepistö, G. Kostorz, and G. Göltz, Acta Metall. **29**, 969 (1981).
[47] W. Kienzle and W. Frank, Phys. Status Solidi B **124**, 69 (1984).
[48] G. Saada, Acta Metall. **9**, 166 (1961); **9**, 965 (1961).
[49] U. Eßmann, Phys. Solid State **12**, 707 (1965); **12**, 723 (1965).
[50] J.W. Steeds, Proc. R. Soc. London, Ser. A **292**, 343 (1966).
[51] S.J. Basinski and Z.S. Basinski, in *Dislocations in Solids*, edited by F.R.N. Nabarro (North-Holland, Amsterdam, 1979), Vol. 4, p. 261.
[52] L.P. Kubin and B. Devincre, in *Proceedings of the 20th Risø International Symposium on Materials Science: Deformation-Induced Microstructures: Analysis and Relation to Properties*, edited by J.B. Bilde-Sørensen, J.V. Carstensen, N. Hansen, D. Juul Jensen, T. Leffers, W. Pantleon, O.B. Pedersen, and G. Winther (Risø National Labaratory, Roskilde, Denmark, 1999), p. 61.
[53] W. Kleinert and R. Franke, Phys. Status Solidi A **53**, K177 (1979).
[54] P. Alexopoulos and J.G. Byrne, Metall. Trans. A **9**, 1829 (1978).
[55] T.L. Grobstein, S. Sivashankaran, G. Welsch, N. Panigrahi, J.D. McGervey, and J.W. Blue, Mater. Sci. Eng., A **138**, 191 (1991).
[56] K.G. Lynn, C.M. Wan, R.W. Ure, and J.G. Byrne, Phys. Status Solidi A **22**, 731 (1974).
[57] W.B. Gauster, W.R. Wampler, W.B. Jones and J.A. van den Avyle, in *Proceedings of the 5th International Conference on Positron Annihilation* (Ref. 25), p. 125.
[58] J.H. Hartley, R.H. Howell, P. Asoka-Kumar, P.A. Sterne, D. Akers, and A. Denison, Appl. Surf. Sci. **149**, 204 (1999).
[59] A. Barbieri, S. Hansen-Ilzhöfer, A. Ilzhöfer, and U. Holzwarth, Appl. Phys. Lett. **77**, 1911 (2000). Due to a calibration error after repairing the amplitude controller of the Instron 1273 the stress amplitudes we reported in this publication are 10 MPa too high. However, this does not affect the conclusions presented there.
[60] K.G. Lynn and J.G. Byrne, Metall. Trans. A **7**, 604 (1976).
[61] M. Gerland, B. Ait Saadi, and P. Violan, Mater. Sci. Eng. **96**, L1 (1987).
[62] M. Gerland, J. Mendez, P. Violan, and B. Ait Saadi, Mater. Sci. Eng., A **118**, 83 (1989).
[63] J.-B. Vogt, Ph.D. thesis, Universite de Lille, 1991.
[64] K. Obrtlík, T. Kruml, and J. Polák, Mater. Sci. Eng., A **187**, 1 (1994).
[65] Y. Li and C. Laird, Mater. Sci. Eng., A **186**, 65 (1994).
[66] Y. Li and C. Laird, Mater. Sci. Eng., A **186**, 87 (1994).
[67] U. Holzwarth, A. Barbieri, S. Hansen-Ilzhöfer, P. Schaaff, and M.

Haaks, Appl. Phys. A: Mater. Sci. Process. **73**, 467 (2001).
[68] S. Hansen, U. Holzwarth, M. Tongbhoyai, T. Wider, and K. Maier, Appl. Phys. A: Mater. Sci. Process. **65**, 47 (1997).
[69] Y. Kawaguchi and Y. Shirai, J. Nucl. Sci. Technol. **39**, 1033 (2002).
[70] Y. Kawaguchi, N. Nakamura, and S. Yusa, J. Jpn. Inst. Met. **66**, 740 (2002).
[71] Y. Kawaguchi, N. Nakamura, and S. Yusa, Mater. Trans., JIM **43**, 727 (2002).
[72] Y. Kawaguchi and N. Nakamura, J. Jpn. Inst. Met. **65**, 835 (2001).
[73] B. Somieski, R. Krause-Rehberg, H. Salz, and N. Meyendorf, J. Phys. IV **5**, C1-127 (1995).
[74] M.T. Hutchings, D.J. Buttle, R. Colbrook, W. Dalzell, and C.B. Scruby, J. Phys. IV **5**, C1-111 (1995).
[75] M. Uchida, N. Nakamura, Y. Obta, and K. Yoshida, Ishikawajima-Harima Eng. Rev. **35**, 260 (1995).
[76] L. Pryce and K.W. Andrews, J. Iron Steel Institute **196**, 415 (1960).
[77] *Annual Book of ASTM Standards, Metals Test Methods and Analytical Procedures* (American Society for Testing and Materials, Philadelphia, PA, 1992), Vol. 03.01.
[78] A.E. Waltar and A.B. Reynolds, *Fast Breeder Reactors* (Pergamon Press, New York, 1981).
[79] R.W. Siegel, J. Nucl. Mater. **69&70**, 117 (1978).
[80] P. Erhardt, in *Numerical Data and Functional Relationships in Science and Technology*, edited by H. Ullmaier, Landolt-Börnstein, New Series, Group III, Vol. 25 (Springer-Verlag, Berlin, 1990), p. 88 and 345.
[81] T.M. Wang, B.Y. Wang, S.H. Zhang, and M. Doyama, Mater. Sci. Forum **105-110**, 1321 (1992).
[82] U. Holzwarth, H. Stamm, J.D. Boerman, and S. Colpo (unpublished).
[83] A.H. Cottrell, in *Theory of Crystal Dislocations* (Gordon and Breach, New York, London, 1964).
[84] H. Mughrabi, Mater. Sci. Rep. **33**, 207 (1978).
[85] *Table of Isotopes*, 7th ed., edited by C.M. Lederer and V.S. Shirley (Wiley, New York, 1978).
[86] B. Somieski, T.E.M. Staab, and R. Krause-Rehberg, Nucl. Instrum. Methods Phys. Res. A **381**, 128 (1996).
[87] *Metals Handbook*, 9th ed., *Vol. 3: Properties and Selection: Stainless Steels, Tool Materials and Special Purpose Metals* (American Society for Metals, Metals Park, Ohio, 1980).
[88] S. Kupca, D.P. Kerr, B.G. Hoog, and Z.S. Basinski, Can. J. Phys. **60**, 201 (1982).
[89] E. Kuramoto, V. Novak, and V. Paidar, Scr. Metall. Mater. **26**, 557 (1992).
[90] L.P. Karjalainen, M. Moilanen, R. Myllylä, and K. Palomäki, Phys. Status Solidi A **62**, 597 (1980).
[91] K. Bennewitz, M. Haaks, T. Staab, S. Eisenberg, T. Lampe, K. Maier, and Z. Metallkde, Z. Metallkd. **93**, 778 (2002).
[92] D. Rönnpagel and Ch. Schwink, Acta Metall. **26**, 319 (1978).
[93] M.B. Bever, D.L. Holt and A.L. Titchener, in *Progress in Materials Science*, edited by B. Chalmers, J.W. Christian, and T.B. Massalski (Pergamon Press, Oxford, 1974), Vol. 17.
[94] A. Seeger and W. Frank, Solid State Phys. **3&4**, 125 (1988).
[95] A rather complete synopsis of experimental techniques in observing dislocations and of dislocation concepts may be found in the series *Dislocations in Solids*, edited by F.R.N. Nabarro (North Holland, Amsterdam, 1983).
[96] U. Holzwarth and U. Essmann, Appl. Phys. A: Solids Surf. **57**, 206 (1993); **58**, 197 (1994).
[97] U. Essmann and K. Differt, Mater. Sci. Eng., A **208**, 56 (1996).
[98] A. van den Beukel, in *Vacancies and Interstitials in Metals*, edited by A. Seeger, D. Schuhmacher, W. Schilling, and J. Diehl (North-Holland, Amsterdam, 1970), p. 42.
[99] G. Saada, in *Proceedings of the 20th Risø International Symposium on Materials Science: Deformation-Induced Microstructures: Analysis and Relation to Properties* (Ref. 52), p. 147.
[100] R.E. Schramm and R.P. Reed, Metall. Trans. A **6**, 1345 (1975).
[101] C. Corbel, M.J. Puska, and R.M. Nieminen, in *Positron Annihilation*, edited by P.C. Jain, R.M. Singru, and K.P. Gopinathan (World Scientific, Singapore, 1985), p. 576.
[102] H. Greif, M. Haaks, U. Holzwarth, U. Männig, M. Tongbhoyai, T. Wider, K. Maier, J. Bihr, and B. Huber, Appl. Phys. Lett. **71**, 2115 (1997).
[103] A. David, G. Kögel, P. Sperr, and W. Triftshäuser, Phys. Rev. Lett. **87**, 067402 (2001).